Published by Institute of Physics Publishing for SISSA/ISAS
Received: *July 11, 2002*
Accepted: *July 25, 2002*

CP-violating effects in neutralino scattering and annihilation

Paolo Gondolo*

Max Planck Institut für Physik
Föhringer Ring 6, 80805 Munich, Germany
E-mail: gondolo@mppmu.mpg.de

Katherine Freese

Physics Department, University of Michigan
Ann Arbor, MI 48109, USA
E-mail: ktfreese@umich.edu

Abstract: CP-violating effects that mix the CP-even and CP-odd Higgs bosons can have important consequences for annihilation and scattering of supersymmetric neutralino dark matter. Specifically, we study the dependence on the phase of the third generation trilinear couplings A_t and A_b. We find enhancements in the neutralino annihilation scattering rate which are typically factors of one to four; in the narrow regime of parameter space with neutralino mass close to half the Higgs mass, we find new (CP violating) resonances which may increase the annihilation cross section by factors up to 10^6. CP-violating effects can also modify the neutralino scattering rate off nucleons. For cross sections accessible to upcoming experiments, the rate can be enhanced by a factor as large as 2 or suppressed by a factor of up to 3; for lower cross sections, the suppression can be as large as seven orders of magnitude. We find cases in the region being probed by dark matter searches which are experimentally or cosmologically excluded when CP is conserved but are allowed when CP is violated. These effects are important for direct and indirect detection of neutralino dark matter in cryogenic detectors, the Earth, the Sun, the galactic halo and the galactic center.

Keywords: Cosmology of Theories beyond the SM, Dark Matter.

*Current address is Department of Physics, Case Western Reserve University, 10900 Euclid Ave, Cleveland, OH 44106, USA. E-mail: pxg26@po.cwru.edu.

http://jhep.sissa.it/archive/papers/jhep072002052/jhep072002052.pdf

JHEP07(2002)052

Contents

1. Introduction

The nature of the dark matter in the universe is one of the outstanding questions in astro/particle physics. One of the favored candidates is the lightest supersymmetric (SUSY) particle. Such a particle is weakly interacting and massive (with mass in the range 1 GeV–few TeV), and hence is frequently characterized as a WIMP (weakly interacting massive particle). In the minimal supersymmetric standard model (MSSM), the lightest SUSY particle in most cases is the lightest neutralino, a linear combination of the supersymmetric partners of the photon, Z^0 boson, and neutral-Higgs bosons,

$$\tilde{\chi}_1^0 = N_{11}\widetilde{B} + N_{12}\widetilde{W}^3 + N_{13}\widetilde{H}_1^0 + N_{14}\widetilde{H}_2^0 \,, \tag{1.1}$$

where $\widetilde{B}$ and $\widetilde{W}^3$ are the supersymmetric partners of the U(1) gauge field B and of the third component of the SU(2) gauge field W^3 that mix to make the photon and Z^0 boson. (We will also use the letter χ for $\tilde{\chi}^0_1$.)

Much work has been done studying the possibilities for detecting these particles. Possibilities include direct detection [1], whereby the particle interacts with a nucleon in a low temperature detector, and is identified by the keV of energy it deposits in the nucleon; and indirect detection, whereby (1) the particles are captured in the Sun or Earth, sink to the center of the Sun or Earth, annihilate with one another in the core, and give rise to particles including neutrinos which can be detected by experiments on the surface of the Earth [2, 3], or (2) the particles annihilate in the galactic halo [4] or the galactic center [5] and produce anomalous components in the flux of cosmic rays. The interaction processes of the lightest SUSY particle are clearly of great importance in calculations of predicted rates for both direct and indirect detection.

In this paper we discuss some effects of CP violation on the neutralino annihilation and scattering cross sections. The MSSM introduces several new phases in the theory which are absent in the standard model. Supplemented by a universality condition at the grand unification scale, only two of these are independent. In this case, one may choose to work in a basis in which the two non-trivial CP-violating phases reside in μ and the universal soft trilinear coupling A_0 of the Higgs fields to the scalar fermions $\tilde{f}$. Previously Falk, Ferstl and Olive [6] have considered the effect on neutralino cross sections of a non-zero phase of μ, the mixing mass parameter involving the two Higgs chiral superfields in the superpotential. Here, on the other hand, we consider the effect on neutralino cross sections of the case where the soft trilinear scalar couplings A_f are complex numbers, where subscript f refers to the quarks. To be specific, we will take $A \equiv A_t = A_b$ with arbitrary $\arg(A)$, and we take $\mathrm{Im}(\mu) = 0$ and $A_u = A_d = A_c = A_s = A_\ell = 0$ for the first and second generations of squarks and for all sleptons. This type of model with non-universal trilinear couplings are known [7] to be compatible with current upper limits on the electric dipole moments of electrons and neutrons. These constraints would be tighter if one took A_u, A_d or A_ℓ to be non-zero. Let us be very clear that this choice of assumptions about the parameters is *not* motivated by supergravity (SUGRA); the parameters in a SUGRA model would in fact be quite different. Our general intent here is to take a reasonable and simple choice of parameters which will allow us to study aspects of the effects of CP violation.

The phase of A enters into the neutralino cross sections in two places: 1) into the squark masses, and 2) into the Higgs sector. For example, one of the processes that contributes to neutralino annihilation is s-channel exchange of the three neutral Higgs bosons, h, H, and A, into final state fermions (see figure 1). The first two of these neutral Higgs bosons, h and H, are CP even, while A is CP odd. The new aspect considered here is the possibility of mixing between the CP-even Higgs scalars (h and H) and the CP-odd scalar A. This mixing was first studied by Pilaftsis [8], who found that the size of CP violation can be fairly large, i.e. of order one, for a range of kinematic parameters preferred by SUSY. He found that a large HA mixing can naturally occur within two-Higgs doublet models either at the tree level, if one adds softly CP-violating breaking terms to the Higgs potential, or

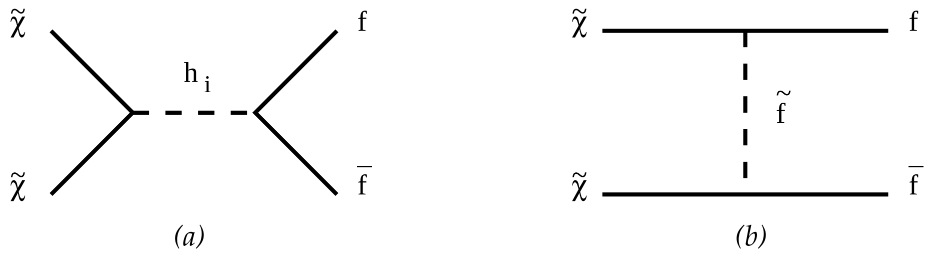

Figure 1: Processes that contribute to neutralino annihilation and scattering and are affected by the CP-violating phase of A. For annihilation: (a) s-channel diagrams via the three neutral Higgs bosons h_1, h_2, and h_3 into final state fermions f, and (b) t-channel diagrams via intermediate squarks $\tilde{f}$ into final state fermions. For scattering: crossed diagrams.

at one loop, after integrating out heavy degrees of freedom that break the CP invariance of the Higgs sector, such as heavy Majorana neutrinos. In any case, in this paper, we consider the one-loop effects of $\mathrm{Im}(A) \neq 0$ on scattering and annihilation cross sections relevant to direct and indirect detection.

Utili/CollapseCitsThe cross section for neutralino annihilation can be enhanced. We find typical enhancements of factors of one to four. In addition, we find new (CP violating) resonances in the cross section for neutralino annihilation that can enhance the annihilation cross section by many orders of magnitude. Without CP violation there are two CP-even Higgs bosons and one CP-odd Higgs boson; ordinarily, in order to conserve CP, two neutralinos can annihilate only via the CP-odd Higgs bosons (at very small relative velocities). Here, however, because of the CP-violating effects that mix the CP-even and CP-odd Higgs bosons, the neutralino can annihilate via any of the three Higgs mass eigenstates. When the annihilation of neutralinos via these new eigenstates is on resonance, large enhancements of the annihilation cross section are possible. We stress that these enormous enhancements only take place for narrow regimes of parameter space when the neutralino mass is close to half the Higgs mass. When the mass is on resonance, we find interesting effects in two different narrow regimes of supersymmetric parameter space: in one regime, we find enhancements of up to 10–100 in the annihilation cross section today without significant changes in the relic density of neutralinos; in the other regime of parameter space, we find enhancements of up to 10^6 in the annihilation cross section. In this second case, models that ordinarily (without CP violation) have too large a relic density to be viable are brought into a reasonable range of density. In addition, their annihilation cross sections, which are ordinarily too low to be experimentally accessible, are enhanced to the accessible range. These same CP-violating effects change the mass of the lightest Higgs boson and can in some cases reduce the neutralino scattering cross section with nucleons by factors of up to 10^{-7}.

In section 2 we discuss our general approach. In section 3, we discuss the squark sector, and in section 4, the Higgs sector. In section 5, we discuss experimental constraints on the parameters. In sections 6 and 7 we give the scattering and annihilation cross sections. In section 8, we present our results and a qualitative discussion of their consequences for neutralino relic density and direct and indirect searches.

2. General approach

The minimal supersymmetric standard model provides a well-defined calculational framework [9], but contains at least 106 yet-unmeasured parameters [10]. Most of them control details of the squark and slepton sectors, and can safely be disregarded in dark matter studies. So similarly to Bergström and Gondolo [11], we restrict the number of parameters to 6 plus one CP-violating phase: the "CP-odd" scalar mass m_A (which in our CP-violating scenario is just a mass parameter), the Higgs mass parameter μ, the gaugino mass parameter M_2 (we impose gaugino mass unification), the ratio of Higgs vacuum expectation values $\tan\beta$, a sfermion mass parameter $\widetilde{M}$ (not to be confused with the sfermion mass, see eqs. (3.2) and (3.5) below), and a complex sfermion mixing parameter $A \equiv A_t = A_b$ for the third generation (we set the A's of the first two generations to zero). The phase of A is the only CP-violating phase we introduce besides the standard model CKM phase.

Note that we have taken a set of restrictive assumptions commonly used [12, 13] in dark matter studies in the context of the MSSM. Namely, a) all trilinear parameters are set to zero except those of the third family, which are unified to a common value at the electroweak scale; b) all squarks and sleptons soft-mass parameters are taken as degenerate at the electroweak scale; c) the gaugino masses are assumed to unify at the unification scale. Let us repeat that this choice of assumptions about the parameters is *not* motivated by supergravity (SUGRA); the parameters in a SUGRA model would in fact be quite different. Our general intent here is to take a reasonable and simple choice of parameters which will allow us to study the possible effects of CP violation. A more complete study of the joint effects of all CP-violating terms is beyond the scope of this paper.

We use the database of points in parameter space built in refs. [11, 14, 15], setting their A_b equal to A_t. Parameter values are chosen at random in the following ranges: $|\mu| < 50\,\mathrm{TeV}$, $|M_2| < 50\,\mathrm{TeV}$, $1 < \tan\beta \leq 60$, $m_A < 10\,\mathrm{TeV}$, $\widetilde{M} < 30\,\mathrm{TeV}$, $|A_t| \leq 3\widetilde{M}$. (Notice that $\widetilde{M}$ is a sfermion mass parameter at the weak scale, see eq. (3.2) below, and that we will limit the neutralino mass $m_\chi < 1\,\mathrm{TeV}$.) There are 132,887 sets of parameter values in the database. Hence we explore a substantial fraction of the supersymmetry parameter space, running through different possible neutralinos as the lightest SUSY particle.

We modify the squark and Higgs couplings in the neutralino dark matter code DarkSUSY [16] to include a non-zero phase of A. We also add all diagrams that contribute to neutralino scattering and annihilation and would vanish when CP is conserved.

To investigate the effects of the phase of A, we perform the following procedure. For each of the 132,887 sets of parameter values in the database, we run through 50 values of the phase of A, so that we effectively explore $50 \times 132,887 \sim 6.6 \times 10^6$ models. We loop over a circle with $\arg(A)$ varying from 0 to 2π. At each point, we check bounds on the electric dipole moment, on the Higgs mass, on other particle masses, on the $b \to s\gamma$ branching ratio, and on the invisible Z width (table 1 gives a listing of the bounds we apply). If any of these bounds are violated, we move to the next point on the circle. If all the bounds are satisfied, we calculate the spin-independent neutralino–proton scattering cross section $\sigma_{\chi p}$. We record the two values of the phase of A where $\sigma_{\chi p}$ is highest and lowest, respectively, with the bounds satisfied. Then, once we have looped through all the possible values for the phase of A, we have found the two points with the maximum enhancement and suppression of the scattering cross section. We then compare with the scattering cross section in the case of no CP violation.

We do the same for the annihilation cross section times relative velocity σv at relative velocity $v = 0$ (we recall that $\sigma \sim 1/v$ as $v \to 0$). Thus we obtain the values of the phase of A where σv is maximum and minimum.

3. Squark sector

The (complex) scalar top and bottom mass matrices can be expressed in the $(\tilde{q}_L, \tilde{q}_R)$ basis as

$$\mathcal{M}^2_{\tilde{q}} = \begin{pmatrix} M^2_{\widetilde{Q}} + m_q^2 + (T_{3q} - e_q \sin^2\theta_W)\cos 2\beta m_Z^2 & m_q\,(A_q^* - \mu R_q) \\ m_q\,(A_q - \mu^* R_q) & M^2_{\widetilde{R}} + m_q^2 + e_q \sin^2\theta_W m_Z^2 \cos 2\beta \end{pmatrix}, \tag{3.1}$$

where $q = t$ or b; $e_t = 2/3$; $e_b = -1/3$; $T_{3t} = 1/2$; $T_{3b} = -1/2$; $R_t = \cot\beta$, $R_b = \tan\beta$; and $M^2_{\widetilde{R}} = M^2_{\widetilde{U}}$ $[M^2_{\widetilde{D}}]$ for t $[b]$. We set

$$M_{\widetilde{Q}} = M_{\widetilde{U}} = M_{\widetilde{D}} = \widetilde{M}\,, \tag{3.2}$$

our sfermion mass parameter. We impose this relation at the electroweak scale. Even in the case of no CP violation, when both μ and A are real, there is mixing between the squarks, and this matrix must be diagonalized to find the mass eigenstates. Here we take A to be complex. Then we obtain the mass eigenstates $\tilde{q}_1, \tilde{q}_2$ from the weak eigenstates $\tilde{q}_L, \tilde{q}_R$ through the rotation

$$\begin{pmatrix} \tilde{q}_1 \\ \tilde{q}_2 \end{pmatrix} = \begin{pmatrix} \cos\theta_{\tilde{q}} & \sin\theta_{\tilde{q}} e^{i\gamma_{\tilde{q}}} \\ -\sin\theta_{\tilde{q}} & \cos\theta_{\tilde{q}} e^{i\gamma_{\tilde{q}}} \end{pmatrix} \begin{pmatrix} \tilde{q}_L \\ \tilde{q}_R \end{pmatrix}, \tag{3.3}$$

where $\gamma_{\tilde{q}} = \arg(A_q^* - \mu R_q)$ and the rotation angle $\theta_{\tilde{q}}$ $(-\pi/4 \le \theta_{\tilde{q}} \le \pi/4)$ may be obtained by

$$\tan(2\theta_{\tilde{q}}) = \frac{2m_q|A_q^* - \mu R_q|}{M^2_{\widetilde{R}} - M^2_{\widetilde{Q}} + (2e_q \sin^2\theta_W - T_{3q}) m_Z^2 \cos 2\beta}\,. \tag{3.4}$$

The masses of $\tilde{q}_1$ and $\tilde{q}_2$ are then given by

$$\begin{aligned} m^2_{\tilde{q}_{1,2}} = \frac{1}{2}\Bigg\{ & M^2_{\widetilde{Q}} + M^2_{\widetilde{R}} + T_{3q} m_Z^2 \cos 2\beta \pm \mathrm{sign}(\theta_{\tilde{q}}) \times \\ & \times \sqrt{\Big[M^2_{\widetilde{R}} - M^2_{\widetilde{Q}} + (2e_q \sin^2\theta_W - T_{3q}) m_Z^2 \cos 2\beta\Big]^2 + 4m_q^2 \left|A_q^* - \mu R_q\right|^2}\,\Bigg\}\,. \end{aligned} \tag{3.5}$$

The $+$ sign is for $\tilde{q}_1$ and the $-$ sign for $\tilde{q}_2$.

The mixing in eq. (3.3) also modifies the squark couplings to the neutralino and the corresponding quark. Writing the relevant interaction term as

$$\mathcal{L}_{\rm int} = \tilde{q}_i \overline{\chi}\left(g^L_{\tilde{q}_i \chi q} P_L + g^R_{\tilde{q}_i \chi q} P_R\right) q + \text{h.c.}\,, \tag{3.6}$$

with $P_L = (1-\gamma_5)/2$, $P_R = (1+\gamma_5)/2$, and $i = 1,2$, we have

$$\begin{pmatrix} g^K_{\tilde{q}_1\chi q} \\ g^K_{\tilde{q}_2\chi q} \end{pmatrix} = \begin{pmatrix} \cos\theta_{\tilde{q}} & \sin\theta_{\tilde{q}} e^{i\gamma_{\tilde{q}}} \\ -\sin\theta_{\tilde{q}} & \cos\theta_{\tilde{q}} e^{i\gamma_{\tilde{q}}} \end{pmatrix} \begin{pmatrix} g_{KL} \\ g_{KR} \end{pmatrix}, \tag{3.7}$$

where $K = L, R$,

$$g_{LL} = -\sqrt{2}\left(T_{3q} g N_{12} + (e_q - T_{3q}) g' N_{11}\right), \qquad g_{RR} = \sqrt{2} e_q g' N_{11}, \tag{3.8}$$

and

$$g_{LR} = g_{RL} = -\frac{g m_u N_{14}}{\sqrt{2} m_W \sin\beta} \tag{3.9}$$

for the up-type quarks,

$$g_{LR} = g_{RL} = -\frac{g m_d N_{13}}{\sqrt{2} m_W \cos\beta} \tag{3.10}$$

for the down-type quarks.

The expressions in this section apply to sleptons provided up-type (s)quarks is replaced with (s)neutrinos and down-type (s)quarks with charged (s)leptons.

4. Higgs sector

4.1 Higgs masses

We evaluate the Higgs boson masses in the effective potential approach. The radiatively corrected Higgs boson mass matrix can be written as

$$\mathcal{M}^2 = \begin{pmatrix} m_Z^2\cos^2\beta + m_A^2\sin^2\beta + \Delta_{11} & -(m_A^2+m_Z^2)\sin\beta\cos\beta + \Delta_{12} & \Delta_{13} \\ -(m_A^2+m_Z^2)\sin\beta\cos\beta + \Delta_{21} & m_Z^2\sin^2\beta + m_A^2\cos^2\beta + \Delta_{22} & \Delta_{23} \\ \Delta_{31} & \Delta_{32} & m_A^2 \end{pmatrix} \tag{4.1}$$

in the basis H_1, H_2, H_3. Here $\Delta_{ij} = \Delta_{ji}$ are the radiative corrections coming from quark and squark loops, with Δ_{13} and Δ_{23} arising from CP violation. We take Δ_{11}, Δ_{12}, and Δ_{22} from ref. [17].

$$\begin{aligned}
\Delta_{11} &= \frac{3g^2}{16\pi^2 m_W^2}\left[\frac{m_b^4}{\cos^2\beta}\left(\ln\frac{m_{\tilde{b}_1}^2 m_{\tilde{b}_2}^2}{m_b^4} + 2Z_b\ln\frac{m_{\tilde{b}_1}^2}{m_{\tilde{b}_2}^2}\right) + \right. \\
&\qquad \left. + \frac{m_b^4}{\cos^2\beta} Z_b^2 g\left(m_{\tilde{b}_1}^2, m_{\tilde{b}_2}^2\right) + \frac{m_t^4}{\sin^2\beta} W_t^2 g\left(m_{\tilde{t}_1}^2, m_{\tilde{t}_2}^2\right)\right], \qquad (4.2) \\
\Delta_{22} &= \frac{3g^2}{16\pi^2 m_W^2}\left[\frac{m_t^4}{\sin^2\beta}\left(\ln\frac{m_{\tilde{t}_1}^2 m_{\tilde{t}_2}^2}{m_t^4} + 2Z_t\ln\frac{m_{\tilde{t}_1}^2}{m_{\tilde{t}_2}^2}\right) + \right. \\
&\qquad \left. + \frac{m_t^4}{\sin^2\beta} Z_t^2 g(m_{\tilde{t}_1}^2, m_{\tilde{t}_2}^2) + \frac{m_b^4}{\sin^2\beta} W_b^2 g(m_{\tilde{b}_1}^2, m_{\tilde{b}_2}^2)\right], \qquad (4.3) \\
\Delta_{12} &= \frac{3g^2}{16\pi^2 m_W^2}\left[\frac{m_t^4}{\sin^2\beta} W_t\left(\ln\frac{m_{\tilde{t}_1}^2}{m_{\tilde{t}_2}^2} + Z_t g(m_{\tilde{t}_1}^2, m_{\tilde{t}_2}^2)\right) + \right. \\
&\qquad \left. + \frac{m_b^4}{\cos^2\beta} W_b\left(\ln\frac{m_{\tilde{b}_1}^2}{m_{\tilde{b}_2}^2} + Z_b g(m_{\tilde{b}_1}^2, m_{\tilde{b}_2}^2)\right)\right], \qquad (4.4)
\end{aligned}$$

where

$$W_q = \frac{\mathrm{Re}(\mu A_q) - |\mu|^2 R_q}{m^2_{\tilde{q}_2} - m^2_{\tilde{q}_1}}\,, \tag{4.5}$$

$$Z_q = \frac{\mathrm{Re}(\mu A_q) R_q - |A_q|^2}{m^2_{\tilde{q}_2} - m^2_{\tilde{q}_1}}\,, \tag{4.6}$$

$$g(m_1^2, m_2^2) = 2 - \frac{m_1^2 + m_2^2}{m_1^2 - m_2^2} \ln \frac{m_1^2}{m_2^2}\,. \tag{4.7}$$

We have rewritten Δ_{13} and Δ_{23} from ref. [8] in a way that shows their proportionality to $\mathrm{Im}(\mu A)$.

$$\begin{aligned}\Delta_{k3} = \frac{3}{16\pi^2} \sum_q g_{A\tilde{q}_1\tilde{q}_1} \Bigg\{ & \frac{1}{2} \left(g_{H_k\tilde{q}_L\tilde{q}_L} + g_{H_k\tilde{q}_R\tilde{q}_R}\right) \log \frac{m^2_{\tilde{q}_1}}{m^2_{\tilde{q}_2}} + \\ & + \Bigg[\sin 2\theta_q \,\mathrm{Re}(e^{i\gamma_q} g_{H_k\tilde{q}_R\tilde{q}_L}) + \\ & + \frac{1}{2} \cos 2\theta_q \left(g_{H_k\tilde{q}_L\tilde{q}_L} - g_{H_k\tilde{q}_R\tilde{q}_R}\right)\Bigg] g\left(m^2_{\tilde{q}_1}, m^2_{\tilde{q}_1}\right) \Bigg\}\,, \end{aligned} \tag{4.8}$$

where the couplings of the Higgs bosons to the squarks are

$$g_{A\tilde{t}_1\tilde{t}_1} = -\frac{g m_t^2}{m_W \sin^2\beta} \frac{\mathrm{Im}(\mu A_t)}{m^2_{\tilde{t}_1} - m^2_{\tilde{t}_2}}\,, \tag{4.9}$$

$$g_{A\tilde{b}_1\tilde{b}_1} = -\frac{g m_b^2}{m_W \cos^2\beta} \frac{\mathrm{Im}(\mu A_b)}{m^2_{\tilde{b}_1} - m^2_{\tilde{b}_2}}\,, \tag{4.10}$$

$$g_{H_1\tilde{t}_L\tilde{t}_L} = -\frac{g m_Z}{\cos\theta_W} \left(T_{3t} - e_t \sin^2\theta_W\right) \cos\beta\,, \tag{4.11}$$

$$g_{H_1\tilde{t}_R\tilde{t}_R} = -\frac{g m_Z}{\cos\theta_W} e_t \sin^2\theta_W \cos\beta\,, \tag{4.12}$$

$$g_{H_1\tilde{t}_R\tilde{t}_L} = \frac{g m_t \mu^*}{2 m_W \sin\beta}\,, \tag{4.13}$$

$$g_{H_1\tilde{b}_L\tilde{b}_L} = -\frac{g m_b^2}{m_W \cos\beta} - \frac{g m_Z}{\cos\theta_W} \left(T_{3b} - e_b \sin^2\theta_W\right) \cos\beta\,, \tag{4.14}$$

$$g_{H_1\tilde{b}_R\tilde{b}_R} = -\frac{g m_b^2}{m_W \cos\beta} - \frac{g m_Z}{\cos\theta_W} e_b \sin^2\theta_W \cos\beta\,, \tag{4.15}$$

$$g_{H_1\tilde{b}_R\tilde{b}_L} = -\frac{g m_b A_b}{2 m_W \cos\beta}\,, \tag{4.16}$$

$$g_{H_2\tilde{t}_L\tilde{t}_L} = -\frac{g m_{b^2}}{m_W \cos\beta} + \frac{g m_Z}{\cos\theta_W} \left(T_{3t} - e_t \sin^2\theta_W\right) \sin\beta\,, \tag{4.17}$$

$$g_{H_2\tilde{t}_R\tilde{t}_R} = -\frac{g m_b^2}{m_W \cos\beta} + \frac{g m_Z}{\cos\theta_W} e_t \sin^2\theta_W \sin\beta\,, \tag{4.18}$$

$$g_{H_2\tilde{t}_R\tilde{t}_L} = -\frac{g m_t A_t}{2 m_W \sin\beta}\,, \tag{4.19}$$

$$g_{H_2\tilde{b}_L\tilde{b}_L} = \frac{g m_Z}{\cos\theta_W}\left(T_{3b} - e_b \sin^2\theta_W\right)\sin\beta\,, \tag{4.20}$$

$$g_{H_2\tilde{b}_R\tilde{b}_R} = \frac{g m_z}{\cos\theta_W} e_b \sin^2\theta_W \sin\beta\,, \tag{4.21}$$

$$g_{H_2\tilde{b}_R\tilde{b}_L} = \frac{g m_b \mu^*}{2 m_W \cos\beta}\,. \tag{4.22}$$

Neglecting D terms, as we should for consistency with the CP-even part and the vertices in our effective potential approach, the corrections Δ_{13} and Δ_{23} simplify to

$$\begin{aligned}\Delta_{13} = \frac{3g^2}{16\pi^2 m_W^2}\Bigg[&\frac{m_b^4}{\cos^3\beta} X_b \left(\ln\frac{m_{\tilde{b}_1}^2}{m_{\tilde{b}_2}^2} + Z_b g\left(m_{\tilde{b}_1}^2, m_{\tilde{b}_2}^2\right)\right) + \\ &+ \frac{m_t^4}{\sin^3\beta} X_t W_t g\left(m_{\tilde{t}_1}^2, m_{\tilde{t}_2}^2\right)\Bigg]\,,\end{aligned} \tag{4.23}$$

$$\begin{aligned}\Delta_{23} = \frac{3g^2}{16\pi^2 m_W^2}\Bigg[&\frac{m_t^4}{\sin^3\beta} X_t \left(\ln\frac{m_{\tilde{t}_1}^2}{m_{\tilde{t}_2}^2} + Z_t g\left(m_{\tilde{t}_1}^2, m_{\tilde{t}_2}^2\right)\right) + \\ &+ \frac{m_b^4}{\cos^3\beta} X_b W_b g\left(m_{\tilde{b}_1}^2, m_{\tilde{b}_2}^2\right)\Bigg]\,,\end{aligned} \tag{4.24}$$

with

$$X_q = \frac{\mathrm{Im}(\mu A_q)}{m_{\tilde{q}_1}^2 - m_{\tilde{q}_2}^2}\,. \tag{4.25}$$

The key thing to notice is that the Δ_{k3} self-energies are proportional to $\mathrm{Im}(\mu A)$. For μ real, they are hence proportional to $\mathrm{Im}(A)$.

We use the effective potential approach to obtain the Higgs masses and couplings. The Higgs mass eigenstates h_i $(i = 1, 2, 3)$ are obtained by diagonalizing the Higgs mass matrix including radiative corrections in eq. (4.1) through the orthogonal Higgs mixing matrix O as

$$h_i = O_{ij} H_j\,. \tag{4.26}$$

In practice, it is convenient to implement the diagonalization in two steps, to separate the CP-violating contributions. First we diagonalize the "CP-even" part through

$$\Phi_i = O^0_{ij} H_j\,, \tag{4.27}$$

where $\Phi_i = H, h, A$ for $i = 1, 2, 3$, respectively. The matrix O^0 would be the Higgs mixing matrix in absence of CP violation

$$O^0 = \begin{pmatrix} \cos\alpha & \sin\alpha & 0 \\ -\sin\alpha & \cos\alpha & 0 \\ 0 & 0 & 1 \end{pmatrix}, \tag{4.28}$$

with

$$\tan(2\alpha) = \frac{2\mathcal{M}_{12}^2}{\mathcal{M}_{11}^2 - \mathcal{M}_{22}^2}\,. \tag{4.29}$$

JHEP07(2002)052

Then we further rotate to the mass eigenstates with an orthogonal matrix O' as

$$h_i = O'_{ij} \Phi_j \tag{4.30}$$

with $O' = OO^{0T}$. This two step procedure allows for a rapid introduction of CP-violating mixing angles for the Higgs sector in the DarkSUSY code.

4.2 Higgs couplings

We will include CP-violating effects by rotating couplings of Higgs particles to other particles as described in this section. In the effective potential approach we neglect vertex corrections. This incorporates the dominant corrections of $\mathcal{O}(g^2 m_t^4/m_W^4)$, and neglects corrections of $\mathcal{O}(g^2 m_t^2/m_W^2)$.

There are terms in the lagrangian that couple the Higgs particles to other particles that are linear in the Higgs fields, for example

$$g_{\Phi_i qq} \Phi_i \bar{q} q = g_{\Phi_i qq} O'_{ji} h_j \bar{q} q \,. \tag{4.31}$$

Terms of this type include coupling to fermions, as shown above, and also terms such as $g_{WH^+\Phi_i} W H^+ \Phi_i$. We will define rotated couplings via

$$g_{h_i ab} = O'_{ij} g_{\Phi_j ab} \,, \tag{4.32}$$

where a and b stand for the appropriate particle name.

Those terms with two Higgs bosons in them, such as

$$g_{Z\Phi_3\Phi_i} Z \Phi_3 \partial_\mu \Phi_i = g_{Z\Phi_3\Phi_i} O'_{k3} O'_{ji} Z h_k \partial_\mu h_j \,, \tag{4.33}$$

must have the couplings rotated with two multiplications by O', e.g.,

$$g_{Zh_k h_j} = g_{ZA\Phi_i} O'_{ji} O'_{k3} - (k \leftrightarrow j) \,. \tag{4.34}$$

Note that, in this particular term, the appropriate antisymmetry properties are maintained, and i takes on values 1 or 2 only.

We have carefully rotated all couplings involving one, two, or three Higgs bosons. It is these rotated couplings that we use in the numerical code (i.e. we replace the ordinary Higgs couplings with these rotated couplings).

As an example, we give the Higgs–quark and Higgs–neutralino vertices that appear in the neutralino–proton spin-independent cross section.

$$g_{h_i uu} = -\frac{g m_u}{2 m_W \sin\beta} \left(O'_{i1} \sin\alpha + O'_{i2} \cos\alpha + O'_{i3} i \cos\beta \right) , \tag{4.35}$$

$$g_{h_i dd} = -\frac{g m_d}{2 m_W \cos\beta} \left(O'_{i1} \cos\alpha - O'_{i2} \sin\alpha + O'_{i3} i \sin\beta \right) , \tag{4.36}$$

$$\begin{aligned} g_{h_i \chi_m \chi_n} = {} & \frac{1}{2} \left(g N^*_{m2} - g' N^*_{m1} \right) \times \\ & \times \Big[N^*_{n3} \left(-O'_{i1} \cos\alpha + O'_{i2} \sin\alpha + O'_{i3} i \sin\beta \right) + \\ & + N^*_{n4} \left(O'_{i1} \sin\alpha + O'_{i2} \cos\alpha - O'_{i3} i \cos\beta \right) \Big] + (m \leftrightarrow n) \,. \end{aligned} \tag{4.37}$$

Here u stands for down-type quarks and neutrinos, d stands for up-type quarks and charged leptons.

Bound	Ref.
$\Gamma_Z^{\rm inv} < 502.4\,{\rm MeV}$	[25]
$m_{H^\pm} > 59.5\,{\rm GeV}$	[26]
$m_{h_i} > 82.5\,{\rm GeV}$	[18]
$m_{\tilde\chi_1^+} > 91\,{\rm GeV}$ if $m_{\tilde\chi_1^0} - m_{\tilde\chi_2^+} > 4\,{\rm GeV}$	[27]
$m_{\tilde\chi_1^+} > 64\,{\rm GeV}$ if $m_{\tilde\chi_1^0} > 43\,{\rm GeV}$ and $m_{\tilde\chi_2^+} > m_{\tilde\chi_2^0}$	[28]
$m_{\tilde\chi_1^+} > 47\,{\rm GeV}$ if $m_{\tilde\chi_1^0} > 41\,{\rm GeV}$	[29]
$m_{\tilde\chi_2^+} > 99\,{\rm GeV}$	[30]
$m_{\tilde\chi_1^0} > 23\,{\rm GeV}$ if $\tan\beta > 3$	[31]
$m_{\tilde\chi_1^0} > 20\,{\rm GeV}$ if $\tan\beta > 2$	[31]
$m_{\tilde\chi_1^0} > 12.8\,{\rm GeV}$ if $m_{\tilde\nu} < 200\,{\rm GeV}$	[32]
$m_{\tilde\chi_1^0} > 10.9\,{\rm GeV}$	[33]
$m_{\tilde\chi_2^0} > 44\,{\rm GeV}$	[34]
$m_{\tilde\chi_3^0} > 102\,{\rm GeV}$	[34]
$m_{\tilde\chi_4^0} > 127\,{\rm GeV}$	[31]
$m_{\tilde g} > 212\,{\rm GeV}$ if $m_{\tilde q_k} < m_{\tilde g}$	[35]
$m_{\tilde g} > 162\,{\rm GeV}$	[36]
$m_{\tilde q_k} > 90\,{\rm GeV}$ if $m_{\tilde g} < 410\,{\rm GeV}$	[37]
$m_{\tilde q_k} > 176\,{\rm GeV}$ if $m_{\tilde g} < 300\,{\rm GeV}$	[35]
$m_{\tilde q_k} > 224\,{\rm GeV}$ if $m_{\tilde g} > m_{\tilde g}$	[38]
$m_{\tilde e} > 78\,{\rm GeV}$ if $m_{\tilde\chi_1^0} < 73\,{\rm GeV}$	[39]
$m_{\tilde\mu} > 71\,{\rm GeV}$ if $m_{\tilde\chi_1^0} < 66\,{\rm GeV}$	[39]
$m_{\tilde\tau} > 65\,{\rm GeV}$ if $m_{\tilde\chi_1^0} < 55\,{\rm GeV}$	[39]
$m_{\tilde\nu} > 44.4\,{\rm GeV}$	[25]
$1\times10^{-4} < {\rm BR}(b\to s\gamma) < 4\times10^{-4}$	[25]
$\lvert d_e\rvert < 0.4\times10^{-26}\,e\,{\rm cm}$	[23]
$\lvert d_n\rvert < 1.79\times10^{-25}\,e\,{\rm cm}$	[24]

Table 1: Experimental bounds we use in this paper. We do not include cosmological bounds nor bounds from dark matter searches.

5. Experimental bounds

5.1 Bounds on masses

We impose experimental bounds on the invisible width of the Z^0 boson, $\Gamma_Z^{\rm inv}$, and on particle masses as listed in table 1.

Since the h, H, and A are rotated into new mass eigenstates bosons, we use the most model independent constraint on the neutral Higgs masses: we take $m_{h_i} > 82.5\,{\rm GeV}$. This constraint was reported by the ALEPH group [18] at the 95% C.L. as a bound on all Higgs masses, independent of $\sin^2(\beta-\alpha)$. Note that this bound, which is a 10% improvement over previous bounds, renders the cross section for direct detection of SUSY particles smaller by a factor of two. This suppression arises because the dominant contribution to the scattering cross section is via Higgs exchange and scales as $\sigma_{\chi p} \propto 1/m_{h_i}^4$.

5.2 Bounds on CP violation

We impose bounds on the branching ratio $\mathrm{BR}(b \to s\gamma)$, and on the electric dipole moments of the electron and of the neutron d_e and d_n.

For $\mathrm{BR}(b \to s\gamma)$ we use the expressions in ref. [19], with inclusion of the one-loop QCD corrections.

Since we assume that the only new CP-violating phase is that of $A \equiv A_b = A_t$, the leading contribution to the electric dipole moment (EDM) arises at two-loops [20]. Chang, Keung, and Pilaftsis [20] have calculated two-loop contributions to the electric dipole moment (EDM) which originate from the potential CP violation due to a non-zero phase of A. We rewrite them showing explicitly their dependence on $\mathrm{Im}(\mu A)$. They find the electric and chromo-electric EDM of a light fermion f at the electroweak scale as

$$\left(d_f^E\right)_{EW} = e e_f \frac{3\alpha_{\rm em}}{64\pi^3} \frac{R_f m_f}{m_A^2} \sum_{q=t,b} \xi_q e_q^2 \left[F\left(\frac{m_{\tilde{q}_1}^2}{m_A^2}\right) - F\left(\frac{m_{\tilde{q}_2}^2}{m_A^2}\right)\right], \tag{5.1}$$

$$\left(d_f^C\right)_{EW} = g_s e_f \frac{\alpha_s}{128\pi^3} \frac{R_f m_f}{m_A^2} \sum_{q=t,b} \xi_q \left[F\left(\frac{m_{\tilde{q}_1}^2}{m_A^2}\right) - F\left(\frac{m_{\tilde{q}_2}^2}{m_A^2}\right)\right], \tag{5.2}$$

where $\alpha_{\rm em} = e^2/(4\pi)$ is the electromagnetic fine structure constant, $\alpha_s = g_s^2/(4\pi)$ is the strong coupling constant, all the kinematic parameters must be evaluated at the electroweak scale m_Z, e_i is the electric charge of particle i, $R_f = \tan\beta$ for $f = u, c, t$, $R_f = \cot\beta$ for $f = e, \mu, \tau, d, s, b$, and $F(z)$ is a two-loop function given by

$$F(z) = \int_0^1 dx \frac{x(1-x)}{z - x(1-x)} \ln\left[\frac{x(1-x)}{z}\right]. \tag{5.3}$$

The EDM of the neutron can then be estimated by a naive dimensional analysis [21, 22] as

$$d_n = \eta^E \, \frac{1}{3}\left(4d_d^E - d_u^E\right) + \eta^C \frac{e}{12\pi}\left(4d_d^C - d_u^C\right). \tag{5.4}$$

We take the numerical values $\eta^E = 1.53$ and $\eta^C = 3.4$ [22].

The CP-violating quantities ξ_t and ξ_b are given by

$$\xi_t = -\frac{g m_t^3 \,\mathrm{Im}(\mu A_t)}{2m_W^2 \sin^2\beta (m_{\tilde{t}_1}^2 - m_{\tilde{t}_2}^2)} \tag{5.5}$$

and

$$\xi_b = -\frac{g m_b^3 \,\mathrm{Im}(\mu A_b)}{2m_W^2 \cos^2\beta (m_{\tilde{b}_1}^2 - m_{\tilde{b}_2}^2)}. \tag{5.6}$$

As an upper bound to the contribution to the measured value of the electron EDM we take $|d_e| < 0.4 \times 10^{-26} e\,\mathrm{cm}$ [23]. The bound on the neutron EDM is $|d_n| < 1.79 \times 10^{-25} e\,\mathrm{cm}$ [24]. We keep only models that satisfy these bounds.

6. Scattering cross section

The neutralino–proton scattering cross section for spin-independent interactions can be written as

$$\sigma_{\chi p} = \frac{G_{\chi p}^2 \mu_{\chi p}^2}{\pi}\,, \tag{6.1}$$

where $\mu_{\chi p} = m_\chi m_p/(m_\chi + m_p)$ is the reduced neutralino–proton mass, and

$$G_{\chi p} = \sum_q \frac{f_q m_p}{m_q} \left[\sum_{i=1}^{3} \frac{\mathrm{Re}(g_{h_i\chi\chi})\,\mathrm{Re}(g_{h_i qq})}{m_{h_i}^2} - \frac{1}{2}\sum_{k=1}^{2} \frac{\mathrm{Re}(g^L_{\tilde{q}_k\chi q} g^{R*}_{\tilde{q}_k\chi q})}{m_{\tilde{q}_k}^2} \right]. \tag{6.2}$$

The sum over q runs over all quarks. The coupling constants are given in eqs. (3.7) and (4.35)–(4.37). We take [40]

$$f_u = 0.023\,, \qquad f_d = 0.034\,, \qquad f_s = 0.14\,, \qquad f_c = f_b = f_t = 0.0595\,, \tag{6.3}$$

and

$$\begin{aligned} m_u &= 5.6\,\mathrm{MeV}, \qquad m_d = 9.9\,\mathrm{MeV}, \qquad m_s = 199\,\mathrm{MeV}\,, \\ m_c &= 1.35\,\mathrm{GeV}\,, \qquad m_b = 5\,\mathrm{GeV}, \qquad m_t = 175\,\mathrm{GeV}\,. \end{aligned} \tag{6.4}$$

The quark mass m_q in the denominator of eq. (6.2) cancels with an identical mass in the numerator coming from the couplings in eqs. (3.4), (3.9), (3.10), (4.35) and (4.35).

Notice that only the real part of the couplings of the Higgs and neutralinos to Higgs bosons in eqs. (4.35)–(4.37) enter the scattering cross section. Since both g_{Aqq} and $g_{A\chi\chi}$ are purely imaginary (because $\mathrm{Im}(\mu) = 0$), introducing a phase in A cannot possibly enhance the Higgs couplings in eq. (6.2). Similarly, the neutralino–squark–quark couplings can only be suppressed for $\mathrm{Im}(A) \neq 0$. However, enhancements to the scattering cross section can still come from the Higgs or squark masses in the denominator in eq. (6.2).

7. Annihilation cross section

The neutralino–neutralino annihilation cross section times relative velocity σv is relevant for neutralino annihilations in the center of the Earth and Sun and in the galactic halo. An enhancement in σv may lead to a higher annihilation signal from the Earth when the capture of neutralinos in the core has not yet reached equilibrium with their self–annihilation. An increased σv gives directly an increased intensity of positron, antiproton, and gamma-ray fluxes from neutralino annihilation in the galactic halo.

The neutralino annihilation cross section also determines the relic density of neutralinos. In this case, there are important contributions at $v \neq 0$ (p-waves, etc.) in large regions of the supersymmetric parameter space. Due to the excessive computational cost of obtaining the relic density in presence of CP violation, in this paper we consider in detail the $v = 0$ case, and postpone a complete study of the effect of CP-violating phases on the neutralino relic density. The enhancements and suppressions of σv at $v = 0$ that we obtain in the following are indications of analogous enhancements and suppressions in the

JHEP07(2002)052

neutralino relic density. In section 8 we present a partial discussion of the expected relic density in those models where we find interesting CP-violating effects.

The annihilation cross section at $v = 0$ includes the following contributions

$$\sigma v = \left[\sum_f \sigma_{\overline{f}f} + \sigma_{W^+W^-} + \sigma_{ZZ} + \sigma_{H^+H^-} + \right.$$
$$\left. + \sigma_{H^+W^-} + \sigma_{H^-W^+} + \sum_{i=1}^{3} \sigma_{h_i Z} + \sum_{ij=1}^{3} \sigma_{h_i h_j} \right] v \,, \tag{7.1}$$

where σ_{XY} refers to the annihilation channel $\chi\chi \to XY$, which is open when $2m_\chi \geq m_X + m_Y$.

The annihilation cross section in each channel can be written in terms of helicity amplitudes $\mathcal{A}$ as

$$\sigma_{XY} v = \frac{\lambda_{XY}}{128\pi m_\chi^2} \sum_{\text{helicities}} |\mathcal{A}|^2, \tag{7.2}$$

where the amplitudes are normalized as in ref. [25] and

$$\lambda_{XY} = \sqrt{\left[1 - \frac{(m_X + m_Y)^2}{4m_\chi^2}\right]\left[1 - \frac{(m_X - m_Y)^2}{4m_\chi^2}\right]}\,. \tag{7.3}$$

The DarkSUSY code already includes analytic expressions for each helicity amplitude required in eq. (7.2), with arbitrary complex couplings between the particles. Hence once we have rotated all vertices as described in section 4, and have added all annihilation diagrams that vanish when CP is conserved (e.g. the s-channel exchange of all Higgs bosons), the annihilation cross section including CP violation is automatically calculated correctly by DarkSUSY.

For future reference, we list the individual contributions to the annihilation cross section including terms that violate CP, although we do not use the following expressions but the amplitudes coded in DarkSUSY.

$$\sigma_{\overline{f}f} v = \frac{N_f \lambda_{ff} m_\chi^2}{32\pi} \left| \sum_{i=1}^{3} \frac{4\,\mathrm{Im}(g_{h_i ff})\,\mathrm{Im}(g_{h_i\chi_1\chi_1})}{m_{h_i}^2 - 4m_\chi^2 - i m_{h_i}\Gamma_{h_i}} + \frac{4 g^A_{Zff}\,\mathrm{Re}(g_{Z\chi_1\chi_1})(m_f/m_\chi)}{m_Z^2} + \right.$$
$$\left. + \sum_{s=1}^{2} \frac{\left(\left|g^R_{\tilde{f}_s\chi f}\right|^2 + \left|g^L_{\tilde{f}_s\chi f}\right|^2\right)(m_f/m_\chi) + 2\,\mathrm{Re}\left(g^L_{\tilde{f}_s\chi f} g^{R*}_{\tilde{f}_s\chi f}\right)}{m_{\tilde{f}_s}^2 + m_\chi^2 - m_f^2 - i m_{\tilde{f}_s}\Gamma_{\tilde{f}_s}} \right|^2 +$$
$$+ \frac{N_f \lambda_{ff}^3 m_\chi^2}{32\pi} \left| \sum_{i=1}^{3} \frac{4i\,\mathrm{Re}(g_{h_i ff})\,\mathrm{Im}(g_{h_i\chi_1\chi_1})}{m_{h_i}^2 - 4m_\chi^2 - i m_{h_i}\Gamma_{h_i}} + \right.$$
$$\left. + \sum_{s=1}^{2} \frac{\left|g^R_{\tilde{f}_s\chi f}\right|^2 - \left|g^L_{\tilde{f}_s\chi f}\right|^2}{m_{\tilde{f}_s}^2 + m_\chi^2 - m_f^2 - i m_{\tilde{f}_s}\Gamma_{\tilde{f}_s}} \right|^2 , \tag{7.4}$$

$$
\begin{aligned}
\sigma_{W^+W^-}v \;=\; & \frac{\lambda_{WW}}{8\pi}\left|\sum_{c=1}^{2}\frac{\lambda_{WW}m_\chi\left(\left|g^R_{W\chi\tilde\chi_c^+}\right|^2+\left|g^L_{W\chi\tilde\chi_c^+}\right|^2\right)+2im_{\tilde\chi_c^+}\,\mathrm{Im}\left(g^L_{W\chi\tilde\chi_c^+}g^{R*}_{W\chi\tilde\chi_c^+}\right)}{m^2_{\tilde\chi_c^+}+m^2_\chi-m^2_W-im_{\tilde\chi_c^+}\Gamma_{\tilde\chi_c^+}}\right|^2+\\
&+\frac{\lambda_{WW}}{4\pi}\left|\sum_{c=1}^{2}\frac{\left[2(m_\chi/m_W)^2-1\right]m_{\tilde\chi_c^+}\,\mathrm{Im}\left(g^L_{W\chi\tilde\chi_c^+}g^{R*}_{W\chi\tilde\chi_c^+}\right)}{m^2_{\tilde\chi_c^+}+m^2_\chi-m^2_W-im_{\tilde\chi_c^+}\Gamma_{\tilde\chi_c^+}}\right|^2, \qquad (7.5)
\end{aligned}
$$

$$
\begin{aligned}
\sigma_{ZZ}v \;=\; & \frac{\lambda_{WW}}{16\pi}\left|\sum_{n=1}^{4}\frac{2\lambda_{ZZ}m_\chi\left|g_{Z\chi\chi_n}\right|^2-2im_{\chi_n}\,\mathrm{Im}(g^2_{Z\chi\chi_n})}{m^2_{\chi_n}+m^2_\chi-m^2_Z-im_{\chi_n}\Gamma_{\chi_n}}\right|^2+\\
&+\frac{\lambda_{WW}}{8\pi}\left|\sum_{n=1}^{4}\frac{\left[2(m_\chi/m_W)^2-1\right]m_{\chi_n}\,\mathrm{Im}\left(g^2_{Z\chi\chi_n}\right)}{m^2_{\chi_n}+m^2_\chi-m^2_Z-im_{\chi_n}\Gamma_{\chi_n}}\right|^2, \qquad (7.6)
\end{aligned}
$$

$$
\begin{aligned}
\sigma_{H^+H^-}v \;=\; & \frac{\lambda_{H^\pm H^\pm}}{8\pi}\left|\sum_{c=1}^{2}\frac{2\,\mathrm{Im}\left(g^L_{H^+\chi_1\chi_c^-}g^{R*}_{H^+\chi_1\chi_c^-}\right)m_{\chi_c^\pm}}{m^2_{\chi_c^\pm}+m^2_\chi-m^2_{H^\pm}-im_{\chi_c^\pm}\Gamma_{\chi_c^\pm}}\right.+\\
&\left.+\sum_{i=1}^{3}\frac{g_{H^+H^-h_i}\,\mathrm{Im}(g_{h_i\chi\chi})}{m^2_{h_i}-4m^2_\chi-im_{h_i}\Gamma_{h_i}}\right|^2, \qquad (7.7)
\end{aligned}
$$

$$
\begin{aligned}
&\sigma_{H^+W^-}v=\sigma_{H^-W^+}v=\\
&=\frac{\lambda^3_{H^\pm W}m^2_\chi}{16\pi m^2_W}\times\\
&\times\left|\sum_{i=1}^{3}\frac{4ig_{Wh_iH^\pm}\,\mathrm{Im}\left(g_{h_i\chi\chi}\right)m_\chi}{m^2_{h_i}-4m^2_\chi-im_{h_i}\Gamma_{h_i}}\right.+ \qquad (7.8)\\
&\left.+\sum_{c=1}^{2}\frac{\left(g^R_{W\chi\tilde\chi_c^+}g^{R*}_{H\chi\tilde\chi_c^+}-g^L_{W\chi\tilde\chi_c^+}g^{L*}_{H\chi\tilde\chi_c^+}\right)m_\chi+\left(g^L_{W\chi\tilde\chi_c^+}g^{R*}_{H\chi\tilde\chi_c^+}-g^R_{H\chi\tilde\chi_c^+}g^{L*}_{H\chi\tilde\chi_c^+}\right)m_{\tilde\chi_c^+}}{m^2_{\tilde\chi_c^+}+m^2_\chi-(m^2_{H^\pm}+m^2_W)/2-im_{\tilde\chi_c^+}\Gamma_{\tilde\chi_c^+}}\right|^2,
\end{aligned}
$$

$$
\begin{aligned}
\sigma_{h_iZ}v \;=\; & \frac{\lambda^3_{h_iZ}m^2_\chi}{16\pi m^2_Z}\left|\sum_{n=1}^{4}\frac{-2\,\mathrm{Re}\left(g_{Z\chi_1\chi_n}g^*_{h_i\chi_n\chi_1}\right)m_\chi+2\,\mathrm{Re}\left(g_{Z\chi_1\chi_n}g_{h_i\chi_n\chi_1}\right)m_{\chi_n}}{m^2_{\chi_n}+m^2_\chi-(m^2_{h_i}+m^2_Z)/2-im_{\chi_n}\Gamma_{\chi_n}}\right.+\\
&\left.+\sum_{j=1}^{3}\frac{4ig_{Zh_ih_j}\,\mathrm{Im}(g_{h_j\chi\chi})m_\chi}{m^2_{h_j}-4m^2_\chi-im_{h_j}\Gamma_{h_j}}-\frac{g_{h_iZZ}\,\mathrm{Re}(g_{Z\chi\chi})}{m^2_Z}\right|^2, \qquad (7.9)
\end{aligned}
$$

$$
\begin{aligned}
\sigma_{h_ih_j}v= & \frac{\lambda_{hA}}{64\pi m^2_\chi S_{ij}}\left|\sum_{n=1}^{4}\frac{4\,\mathrm{Im}\left(g_{h_i\chi_1\chi_n}g^*_{h_j\chi_1\chi_n}\right)m_\chi m_{\chi_n}+\left(m^2_{h_i}-m^2_{h_j}\right)\mathrm{Im}\left(g_{h_i\chi_1\chi_n}g_{h_j\chi_1\chi_n}\right)}{m^2_{\chi_n}+m^2_\chi-(m^2_{h_i}+m^2_{h_j})/2-im_{\chi_n}\Gamma_{\chi_n}}\right.+\\
&\left.+\sum_{k=1}^{3}\frac{2g_{h_ih_jh_k}\,\mathrm{Im}(g_{h_k\chi\chi})m_\chi}{m^2_{h_k}-4m^2_\chi-im_{h_k}\Gamma_{h_k}}+\frac{ig_{Zh_ih_j}\left(m^2_{h_i}-m^2_{h_j}\right)\mathrm{Re}(g_{Z\chi\chi})}{m^2_Z}\right|^2. \qquad (7.10)
\end{aligned}
$$

N_f is 3 for quarks and 1 for leptons, S_{ij} is a symmetry factor equal to 1 for $i \neq j$ and 2 for $i = j$, $g_{h_i ff}$ and $g_{h_i \chi_m \chi_n}$ are given in eqs. (4.35)–(4.37), $g^L_{\tilde{f}\chi f}$ and $g^R_{\tilde{f}\chi f}$ are given in eqs. (3.7)–(3.10), and

$$
\begin{aligned}
g_{Wh_iH^\pm} &= \frac{g}{2}\left[O'_{i1}\sin(\alpha-\beta) + O'_{i2}\cos(\alpha-\beta) + iO'_{i3}\right], && (7.11)\\
g_{h_iZZ} &= \frac{g}{\cos^2\theta_W}\left[O'_{i1}\cos(\beta-\alpha) + O'_{i2}\sin(\beta-\alpha)\right], && (7.12)\\
g_{Zh_ih_j} &= \frac{ig}{2\cos\theta_W}\left[O'_{i1}\sin(\alpha-\beta) + O'_{i2}\cos(\alpha-\beta)\right]O'_{j3} - (i \leftrightarrow j), && (7.13)\\
g^A_{Zff} &= \frac{gT_{3f}}{2\cos\theta_W}, && (7.14)\\
g^L_{W\chi\chi^+_c} &= -\frac{gN_{14}V^*_{c2}}{\sqrt{2}} + gN_{12}V^*_{c1}, && (7.15)\\
g^R_{W\chi\chi^+_c} &= +\frac{gN^*_{13}U_{c2}}{\sqrt{2}} + gN^*_{12}U_{c1}, && (7.16)\\
g_{Z\chi_m\chi_n} &= \frac{g}{2\cos\theta_W}\left[N_{m4}N^*_{n4} - N_{m3}N^*_{n3}\right], && (7.17)\\
g^L_{H^+\chi_n\chi^-_c} &= -\cos\beta\left[gN^*_{n4}V^*_{c1} + \frac{1}{\sqrt{2}}(gN^*_{n2} + g'N^*_{n1})V^*_{c2}\right], && (7.18)\\
g^R_{H^+\chi_n\chi^-_c} &= -\sin\beta\left[gN_{n3}U_{c1} - \frac{1}{\sqrt{2}}(gN_{n2} + g'N_{n1})U_{c2}\right], && (7.19)\\
g_{H^+H^-h_i} &= -gm_W\left[O'_{i1}\cos(\beta-\alpha) + O'_{i2}\sin(\beta-\alpha)\right] + \\
&\quad + \frac{gm_Z\cos 2\beta}{2\cos\theta_W}\left[O'_{i1}\cos(\beta+\alpha) - O'_{i2}\sin(\beta+\alpha)\right], && (7.20)\\
g_{h_ih_jh_k} &= -\frac{gm_Z}{2\cos\theta_W}\left[O'_{i1}\cos(\alpha+\beta) - O'_{i2}\sin(\alpha+\beta)\right] \times \\
&\quad \times \left[\cos 2\alpha(O'_{j1}O'_{k1} - O'_{j2}O'_{k2}) - \sin 2\alpha(O'_{j1}O'_{k2} + O'_{j2}O'_{k1}) - O'_{j3}O'_{k3}\cos 2\beta\right] + \\
&\quad + (\text{cyclic permutations of } i,j,k). && (7.21)
\end{aligned}
$$

Here V and U are the chargino mixing matrices.

For real μ and real gaugino masses, as we assume here, the terms containing $\mathrm{Im}(g^L_{W\chi\tilde{\chi}^+_c} g^{R*}_{W\chi\tilde{\chi}^+_c})$, $\mathrm{Im}(g^L_{H^+\chi_1\chi^-_c} g^{R*}_{H^+\chi_1\chi^-_c})$, and $\mathrm{Im}(g^2_{Z\chi\chi_n})$ in eqs. (7.5)–(7.7) vanish. In addition, when CP is conserved, the H^+H^- annihilation in eq. (7.7) vanishes at $v = 0$.

Notice that in the annihilation into fermion pairs, in the first terms under absolute values in eq. (7.4) (see figure 1a), there can be contributions from all Higgs bosons h_i for which the imaginary part of $g_{h_i\chi\chi}$ is non-zero. Examining eq. (4.37) for the couplings, recalling that the matrix elements O'_{ij} are real and that for real μ and real gaugino masses $N_{1i}N_{1j}$ are also real, we see that the h_i contributes when O'_{i3} is non-zero. In the CP-conserving case, this happens only for $i = 3$, i.e. for the A boson, while with CP violation this occurs also for $i = 1$ and $i = 2$. The annihilation into $f\bar{f}$ then proceeds through exchange of all Higgs bosons, raising the possibility of resonant annihilation when $2m_\chi$ is approximately equal to the mass of any Higgs boson. This phenomenon is peculiar to CP violation. An example is given in figure 9 below.

8. Results

8.1 Results for the elastic scattering cross section

In figure 2 we show the neutralino–proton elastic scattering cross section as a function of neutralino mass for the $\sim 10^6$ values in SUSY parameter space that we consider. There is no CP violation in the lower panel ($\mathrm{Im}\, A = 0$), while CP violation is allowed in the upper panel. Also shown are the present experimental bounds from the DAMA [41] and CDMS [42] collaborations as well as the future reach of the CDMS (Soudan) [43], CRESST [44] and GENIUS [45] experiments. In the upper panel, it is the maximally enhanced cross section (as a function of $\arg(A)$) that is plotted. The red (dark) points refer to those values of parameter space which have the maximum value of the cross section for non zero $\mathrm{Im}(A)$ and which are experimentally excluded at zero $\mathrm{Im}(A)$. The blue (grey) region refers to those values of parameter space which are enhanced when CP violation is included and which are allowed also at zero $\mathrm{Im}(A)$. The green (light grey) empty squares refer to those

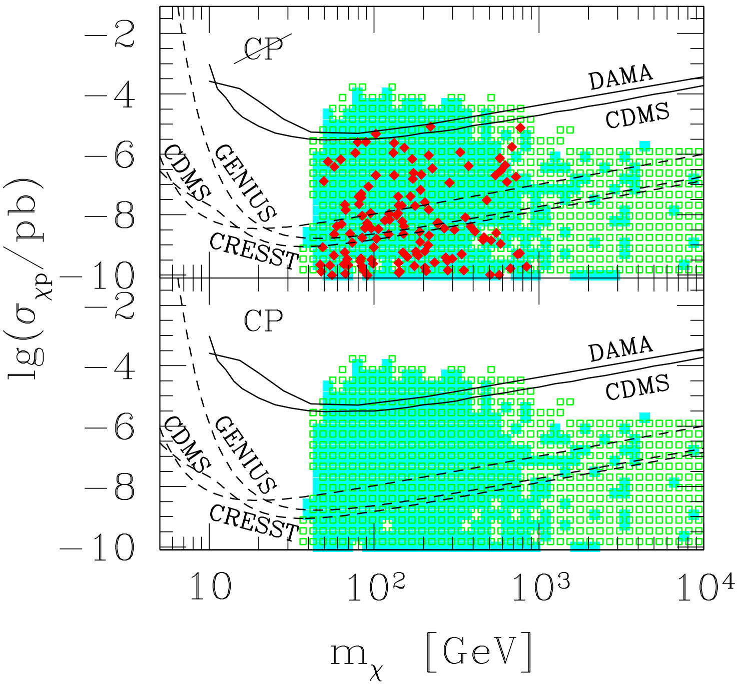

Figure 2: Neutralino elastic scattering cross section (in pb) as a function of neutralino mass (in GeV) for $\sim 10^6$ values in SUSY parameter space. The upper panel is for the case of CP violation via $\mathrm{Im}(A) \neq 0$ while the lower panel is for the case of no CP violation. In the upper panel, it is the maximally enhanced cross section (as a function of $\arg(A)$) that is plotted. The red (dark) points refer to those values of parameter space which have the maximum value of the cross section for non zero $\mathrm{Im}(A)$ and which are experimentally excluded at zero $\mathrm{Im}(A)$. The blue (grey) region refer to those values of parameter space which are enhanced when CP violation is included and which are allowed also at zero $\mathrm{Im}(A)$. The green (light grey) empty squares refer to those values of parameter space which have no enhancement when CP violation is included. The solid lines indicate the current experimental bounds placed by DAMA and CDMS; the dashed lines indicate the future reach of the CDMS (Soudan), GENIUS, and CRESST proposals.

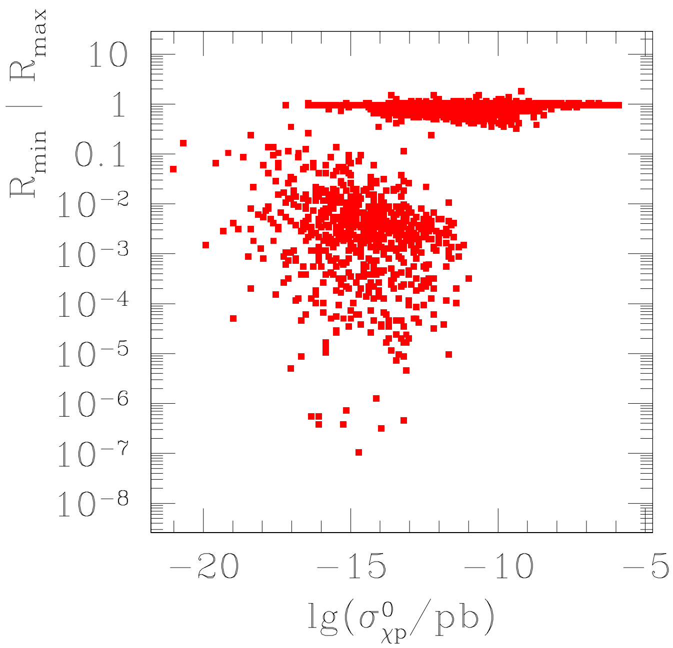

Figure 3: Enhancement and suppression of elastic scattering cross section for the case of CP violating arg(A). The plot shows the ratio $R_{\rm max} = \sigma^{\rm max}/\sigma^0_{\rm max}$ as a function of the unenhanced scattering cross section $\sigma^0_{\rm max} = \max[\sigma(0), \sigma(\pi)]$. Here $\sigma^{\rm max}$ is the enhanced scattering cross section and the superscript max indicates the maximal enhancement as one goes through the phase of A. The denominator of the ratio $R_{\rm max}$ chooses the larger value of the scattering cross section without CP violation, i.e. for phase = 0 or phase = π. Similarly, the ratio $R_{\rm min} = \sigma^{\rm min}/\sigma^0_{\rm min}$ is plotted; this time the denominator chooses the smaller value of the scattering cross section without CP violation, $\sigma^0_{\rm min} = \min[\sigma(0), \sigma(\pi)]$.

values of parameter space which have no enhancement when CP violation is included. From the existence of the red points we conclude that there are indeed points in SUSY parameter space which are ruled out experimentally when CP is conserved but are allowed when CP is violated. By comparing corresponding points in the upper and lower panels of figure 2, we notice that there can be enhancement or suppression of the cross section when we allow for CP violation. There are two types of enhancement: one in which the model without CP violation is allowed and another in which it is experimentally ruled out. In the first case, it is possible to define a ratio between enhanced and unenhanced cross sections, $R_{\rm max} = \sigma^{\rm max}/\sigma^0_{\rm max}$. In the second case, when both $\sigma(0)$ and $\sigma(\pi)$ are excluded, it is not possible to define the previous ratio. Here $\sigma^{\rm max}$ is the maximally enhanced cross section as one goes through the phase of A, and $\sigma^0_{\rm max} = \max[\sigma(0), \sigma(\pi)]$ is the larger of the unenhanced CP conserving cross sections. We plot $R^{\rm max}$ in figure 3 as a function of $\sigma^0_{\rm max}$. In those models in parameter space that we have considered, we notice that the enhancement due to CP violation is at most a factor of two.

In figure 3, we have also plotted the ratio $R_{\rm min} = \sigma^{\rm min}/\sigma^0_{\rm min}$, which is a measure of the maximal suppression of the neutralino–proton cross section when CP violation is included. Here $\sigma^{\rm min}$ is the maximally suppressed cross section as one goes through the phase of A, and $\sigma^0_{\rm min} = \min[\sigma(0), \sigma(\pi)]$ is the smaller of the unenhanced CP conserving cross sections. We

JHEP07(2002)052

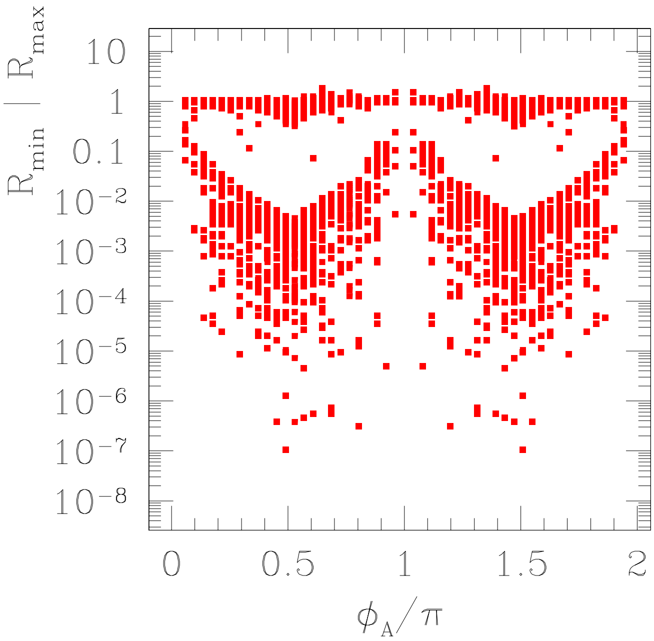

Figure 4: The enhancement/suppression factors $R_{\rm max}$ and $R_{\rm min}$ defined in the caption of figure 3 as a function of the values ϕ_A of the phase of A where the maximum/minimum occur.

see that significant suppression of the scattering cross section, as low as 10^{-7}, is possible, but only for cases which are inaccessible to experiments that will run in the foreseeable future. For cross sections larger than 10^{-10} pb, on the other hand, the suppression is at most a factor of 3.

In figure 4, we show the dependence of these enhancement and suppression factors $R_{\rm max}$ and $R_{\rm min}$ on the phase ϕ_A of A. The points are plotted at those values of ϕ_A at which the maximum or minimum of the scattering cross section occurs. The two populations correspond to the two populations visible in figure 3 at the upper right and the lower left. We have not understood what distinguishes these two populations. Since the large suppressions occur at low values of the unsuppressed scattering cross section, we believe that the large suppressions are due to interference in the scattering amplitude between different Higgs boson exchanges, since these interferences are at the origin of the small unsuppressed cross sections [46].

8.2 Results for the annihilation cross section

We also have obtained values for the neutralino annihilation cross section σv for the case of CP violation through the phase of A. In figure 5 we show the maximum value of σv obtained as we vary ϕ_A as a function of neutralino mass. As in the analogous figure 2 for the scattering cross section, the upper panel includes CP violation while the lower one does not. The distinction between red (dark), blue (grey), and green (light grey) points is as in figure 2.

Figure 6 shows the enhancement of the annihilation cross section via the ratio $R^{\rm ann}_{\rm max} = (\sigma v)^{\rm max}/(\sigma v)^0_{\rm max}$. We see that the annihilation cross section can be significantly enhanced for CP violation with ${\rm Im}(A) \neq 0$. A similar ratio can be constructed for $R^{\rm ann}_{\rm min}$ to show

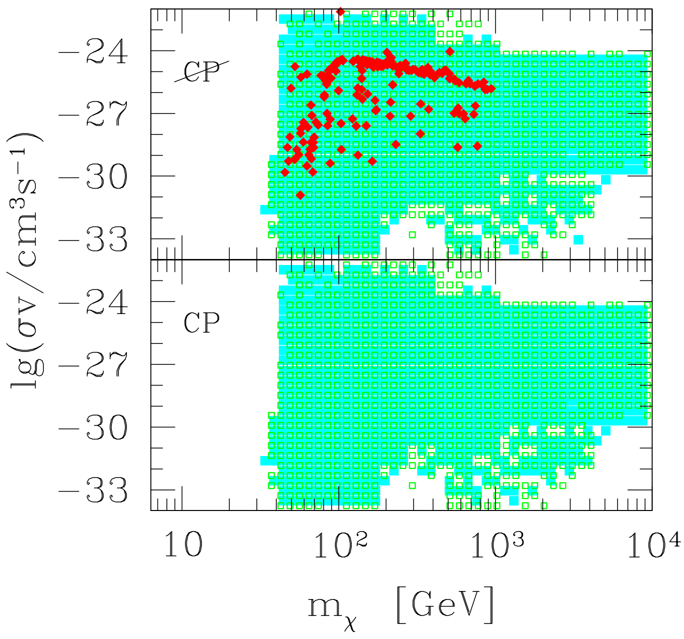

Figure 5: Same as figure 2 but for the neutralino annihilation cross section times relative velocity σv (in cm^3/s at $v = 0$) as a function of neutralino mass (in GeV) for $\sim 10^6$ values in SUSY parameter space.

that the suppression due to CP violation can be roughly a factor of 50. The dependence of these enhancement and suppression factors $R^{\mathrm{ann}}_{\mathrm{max}}$ and $R^{\mathrm{ann}}_{\mathrm{min}}$ on ϕ_A are plotted in figure 7. We have used color coding in figures 6 and 7 to differentiate between resonant and non-resonant cases. Resonances are defined to be those points with neutralino mass satisfying $2m_\chi - m_h < 5 \times 10^{-3} m_h$ where m_h is any of the Higgs masses. Those cases without resonance are shaded (green) and have typical enhancements by factors of one to four, although the enhancement can be as large as a few hundred. These non-resonant cases are perhaps the most interesting as they span a broader regime of SUSY parameter space. In all models for which we find an enhancement in the annihilation cross section of at least 10^3, the enhancement is due to an s-channel resonance with the exchange of one of the Higgs bosons h_1, h_2 or h_3. In the resonant cases (dark points in figure 7, color coded red), the enhancement can be as large as 10^6; however, again we stress that the resonant cases only occur for a very small regime of parameter space in which the neutralino mass is close to half the Higgs mass. See figure 9 for an example of a resonant case.

8.3 Phase dependence of the results

In the four panels in each of the figures 8–12 we display the behavior of the scattering cross section $\sigma_{\chi p}$, the annihilation cross section σv, the branching ratio $\mathrm{BR}(b \to s\gamma)$, and the lightest Higgs boson mass m_{h_1} as a function of the phase ϕ_A of A. In the third and fourth panels we hatch the regions currently ruled out by accelerator experiments. In all four panels we denote the part of the curves that is experimentally allowed by thickened solid lines, and the part that is experimentally ruled out (as seen e.g. in the third and fourth panels) by thinner solid lines.

JHEP07(2002)052

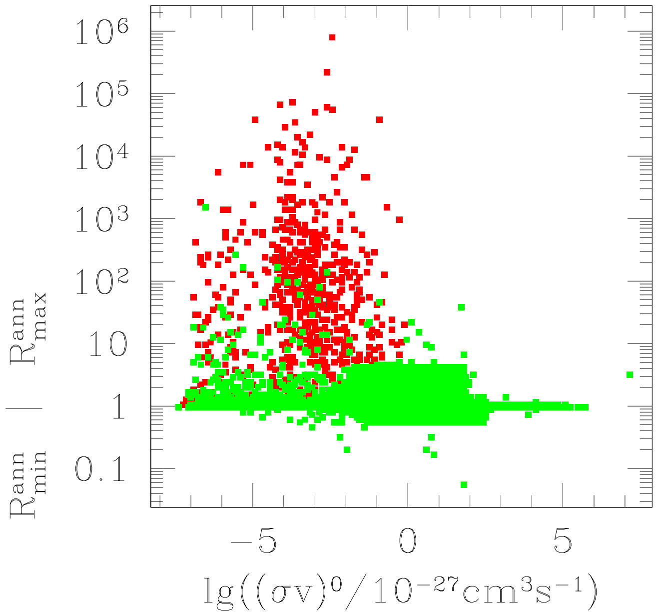

Figure 6: Enhancement and suppression of neutralino annihilation cross section for the case of CP violating arg(A). The plot shows the ratio $R^{\rm ann}_{\rm max} = (\sigma v)^{\rm max}/(\sigma v)^0_{\rm max}$ as a function of the unenhanced annihilation cross section $(\sigma v)^0_{\rm max} = \max[\sigma v(0), \sigma v(\pi)]$. Here $(\sigma v)^{\rm max}$ is the enhanced scattering cross section and the superscript max indicates the maximal enhancement as one goes through the phase of A. The denominator of the ratio $R^{\rm nn}_{\rm max}$ chooses the larger value of the scattering cross section without CP violation, i.e. for phase = 0 or phase = π. Similarly, the ratio $R^{\rm ann}_{\rm min} = (\sigma v)^{\rm min}/(\sigma v)^0_{\rm min}$ is plotted. Here $(\sigma v)^0_{\rm min} = \min[\sigma v(0), \sigma v(\pi)]$. We have used color coding to differentiate between resonant and non-resonant cases. Resonances are defined to be those points with neutralino mass satisfying $2m_\chi - m_h < 5 \times 10^{-3} m_h$ where m_h is any of the Higgs masses. Those cases without resonance are shaded (green) and have typical enhancements by factors of one to four, although the enhancement can be as large as a few hundred. In the resonant cases (the dark points which are color-coded red), the enhancement can be as large as 10^6.

For the models shown in figures 8–12, we give the values of the input parameters and of the neutralino mass and composition (gaugino fraction $|N_{11}|^2 + |N_{12}|^2$) in table 2.

In the case plotted in figure 8, the possible phases are bound by the limit on the $b \to s\gamma$ branching ratio. In the allowed regions, the scattering cross section at CP-violating phases is suppressed, while the annihilation cross section is enhanced. The latter takes its maximum allowed value when the $b \to s\gamma$ limit is reached.

Figure 9 presents another case in which the phase of A is bounded by the $b \to s\gamma$ branching ratio. Here the scattering cross section is enhanced by only 2%, while the annihilation cross section is enhanced by a factor of $\simeq 222$ at $\phi_A \simeq 0.129\pi$. This is due to a resonant annihilation of the neutralinos through s-channel exchange of the h_1 Higgs boson (figure 1a), which occurs when $2m_\chi = m_{h_1}$ (see the lowest panel). Notice that in the CP-conserving case, the s-channel exchange of the CP-even h_1 boson vanishes at $v = 0$ because for real $\chi\chi h_1$ couplings the amplitude is proportional to $\overline{\chi}\chi$ which is zero at $v = 0$. In presence of CP violation, the $\chi\chi h_1$ couplings are in general complex, and the amplitude contains a contribution from $\overline{\chi}\gamma_5\chi$ which does not vanish at $v = 0$. So the h_1 resonant annihilation seen in figure 9 is only possible when CP is violated.

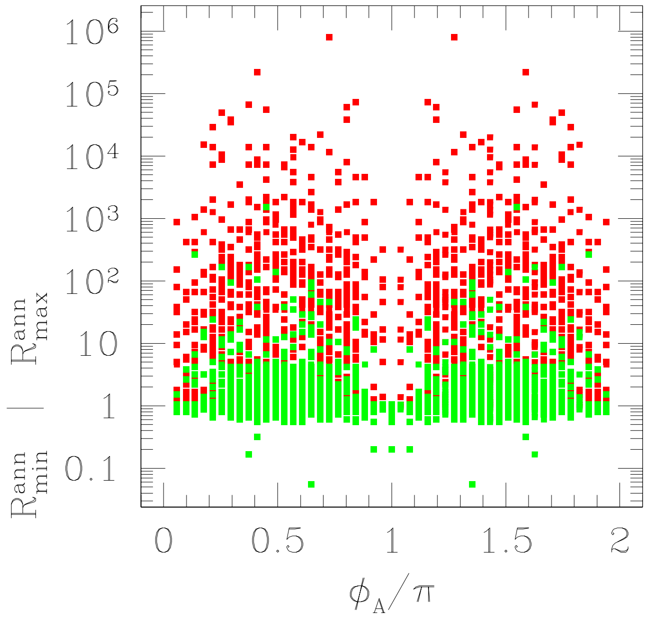

Figure 7: The enhancement/suppression factors $R^{\rm ann}_{\rm max}$ and $R^{\rm ann}_{\rm min}$ defined in the caption of figure 6 as a function of the values ϕ_A of the phase of A where the maximum/minimum occur. As in figure 6, we have used color coding to differentiate between resonant and non-resonant cases. Those cases without resonance are shaded (green) and have typical enhancements by factors of one to four, although the enhancement can be as large as a few hundred. In the resonant cases, the dark points (which are color coded red), the enhancement can be as large as 10^6; however, again we stress that the resonant case only occurs for a very small regime of parameter space in which the neutralino mass is very close to half the Higgs mass.

Figures 10 and 11 show two typical non-resonant cases which are experimentally allowed for all values of the phase ϕ_A. In figure 10, the maximum of the scattering cross section takes place at the CP-conserving value $\phi_A = \pi$ and the minimum at $\phi_A = 0$. On the other hand, here CP violation enhances the annihilation cross section, as can be seen in the second panel. Notice that its maximum occurs at $\phi_A = 0.41\pi$, which is not the point of maximal CP violation $\phi_A = \pi/2$. In figure 11, the annihilation cross section is enhanced by a factor of 4.5 and the scattering cross section is in the region accessible to future dark matter experiments.

Finally figure 12 displays an example in which both CP-conserving cases are experimentally excluded while some CP-violating cases are allowed. This is one of the red (dark) points in figures 2 and 5. The $\phi_A = 0$ case is ruled out by the bounds on both ${\rm BR}(b \to s\gamma)$ and the Higgs mass, the $\phi_A = \pi$ case by only the bound on the Higgs mass. Notice that the scattering cross section is of the order of 10^{-6} pb, in the region probed by the direct detection experiments. The annihilation cross section peaks at $\phi_A = 3\pi/4$; notice that again this value is not the point of maximal CP violation $\phi_A = \pi/2$.

8.4 Consequences for relic abundance and direct and indirect detection rates

In this paper we have calculated the effects of some CP-violating phases on the cross

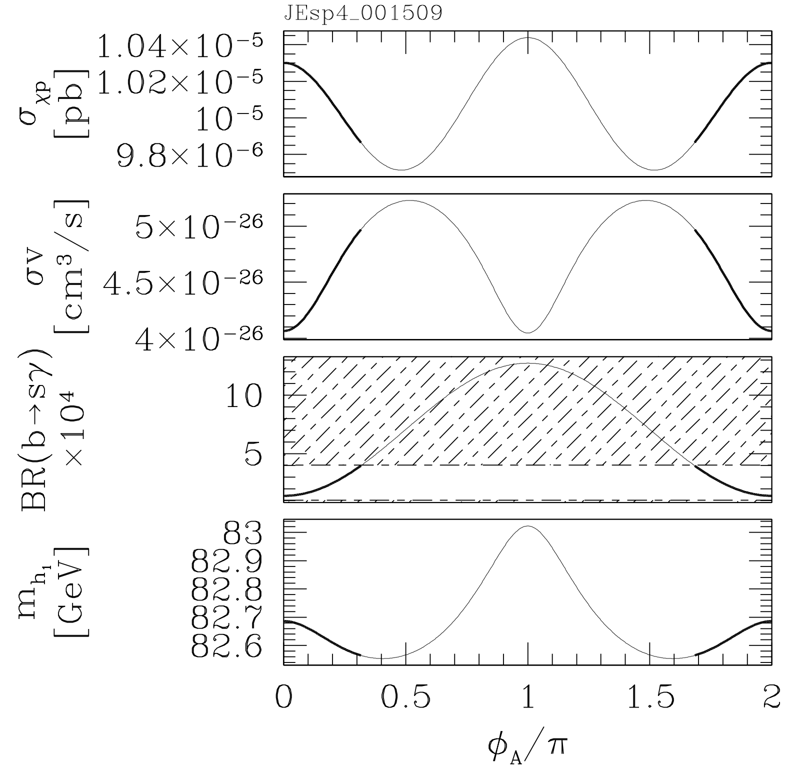

Figure 8: The four panels from top to bottom display the following: the scattering cross section $\sigma_{\chi p}$ in pb, the annihilation cross section σv in cm^3/s, the branching ratio $\mathrm{BR}(b \to s\gamma) \times 10^4$, and the lightest Higgs boson mass m_{h_1} in GeV as a function of the phase ϕ_A of A. CP-conserving phases are $\phi_A = 0, \pi$ while all other values are CP violating. In the third and fourth panels we hatch the regions currently ruled out by accelerator experiments. In all four panels we denote the part of the curves that is experimentally allowed by thickened solid lines, and the part that is experimentally ruled out by thinner solid lines. In this figure, the possible phases are bound by the limit on the $b \to s\gamma$ branching ratio. In the allowed regions, the scattering cross section at CP-violating phases is suppressed, while the annihilation cross section is enhanced. The latter takes its maximum allowed value when the $b \to s\gamma$ limit is reached.

sections for neutralino scattering and annihilation. In this section we discuss in a qualitative way how we expect the relic density and the direct and indirect detection rates to change. Computations required for a detailed evaluation of these changes will be done in a future work.

8.4.1 Relic abundance

As shown in figure 9, we have found large enhancements of the neutralino annihilation cross section today when there is a resonance, $2m_\chi = m_R$, where m_R is the mass of a Higgs boson. The first concern is that when the annihilation cross section is greatly enhanced, the relic density of neutralinos will be greatly suppressed to the point where the models are no longer of cosmological interest. Instead, we will show that there are two interesting regimes of parameter space. In the first, the relic density is relatively unaffected while the

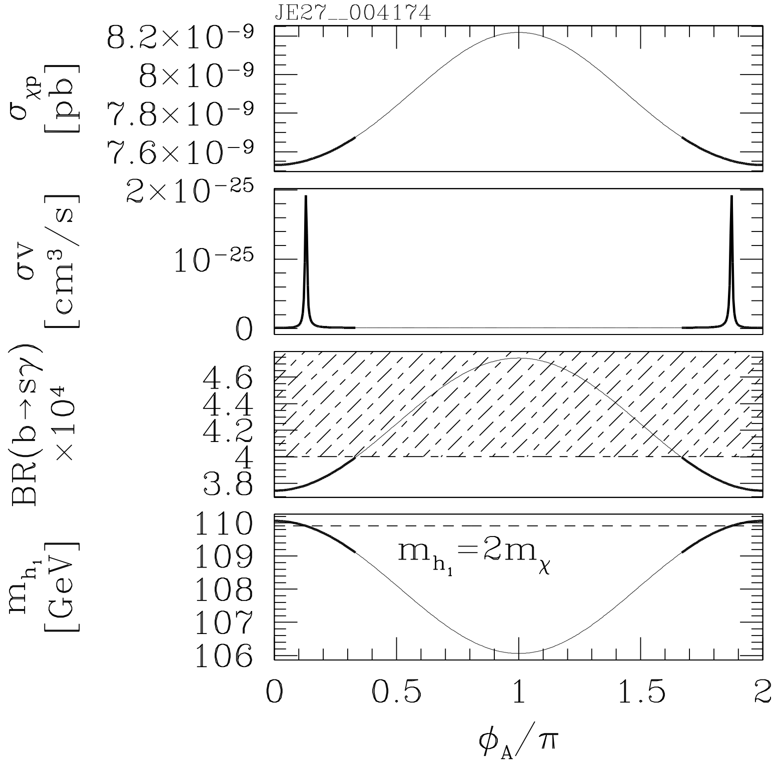

Figure 9: Same notation as figure 8. The phase of A is bounded by the $b \to s\gamma$ branching ratio, the scattering cross section is enhanced by only 2%, and the annihilation cross section is enhanced by a factor of $\simeq 222$ at $\phi_A \simeq 0.129\pi$, where the annihilation proceeds through the h_1 resonance at $2m_\chi = m_{h_1}$ (see bottom panel).

	JEsp4_001509 Figure 8	JE27__004174 Figure 9	JE28__002656 Figure 10	JE26__018457 Figure 11	JEsp4_002809 Figure 12
μ [GeV]	-331.433	-271.973	-234.128	6261.94	958.213
M_2 [GeV]	390.064	106.141	338.688	12462.7	-153.256
m_A [GeV]	84.2527	168.935	325.691	247.150	106.804
$\tan\beta$	31.6126	4.37629	1.80096	23.9737	48.4750
$\widetilde{M}$ [GeV]	1085.05	494.379	1856.43	12168.8	890.647
$A/\widetilde{M}$	2.71920	0.661158	1.88819	-2.42997	-2.05440
m_χ [GeV]	191.46	54.95	172.4	6235.	77.04
$\lvert N_{11}\rvert^2 + \lvert N_{12}\rvert^2$	0.9459	0.9806	0.9571	0.4092	0.99786

Table 2: Model parameters and neutralino mass and composition (gaugino fraction) for the examples in figures 8–12.

annihilation cross section grows by a factor of up to 100. In the second, the relic density is indeed reduced by factors of up to 10^5 while the annihilation cross section is increased by factors which are an order of magnitude higher. In this latter case, models which previously had $\Omega_\chi \sim 10^4$ are brought to cosmologically viable values of $\Omega_\chi \sim 0.1$. Here $\Omega_\chi = \rho_\chi/\rho_c$ is the ratio of the neutralino energy density to the energy density required to close the

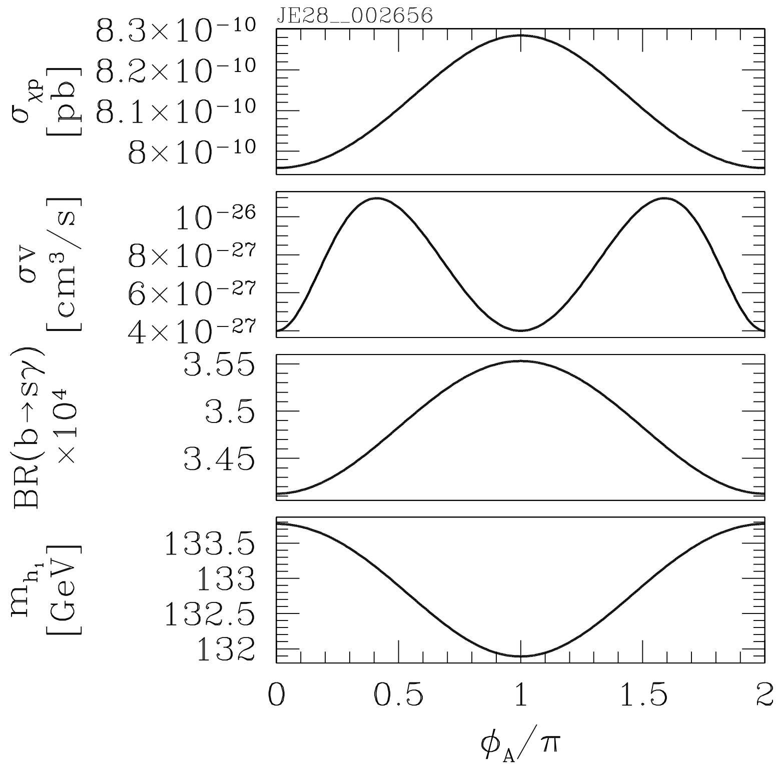

Figure 10: "*The Duck.*" Same notation as figure 8. This case is experimentally allowed for all values of the phase ϕ_A. The maximum of the scattering cross section takes place at the CP-conserving value $\phi_A = \pi$ and the minimum at $\phi_A = 0$. The annihilation cross section is enhanced by CP violation, as can be seen in the second panel.

universe, $\rho_c = 1.88 \times 10^{-29} h_0^2 \,\mathrm{g\,cm}^{-3}$.

We now explain the relationship between the annihilation cross section and the relic density close to a resonance. The neutralino relic density has been widely discussed in the literature. The relic abundance is found by solving the Boltzmann equation for the evolution of the neutralino number density. Here we use a simple and accurate approximation for the relic neutralino density,

$$\Omega_\chi h^2 = \frac{1.02 \times 10^{-27} \,\mathrm{cm}^3/\mathrm{s}}{J g_*^{1/2}} \,, \tag{8.1}$$

where g_* is the number of effectively relativistic degrees of freedom at the time of freeze-out, when the neutralino reaction rate is no longer fast enough to maintain equilibrium. Defining an inverse temperature

$$x = m/T \,, \tag{8.2}$$

we will take $x_f = m/T_f = 25$ as a rough estimate of the freeze-out temperature, a number accurate enough for our purposes. The integral J (which expresses the efficiency of post-freeze-out annihilation) is defined as

$$J = \int_{x_f}^{\infty} \frac{\langle \sigma v \rangle}{x^2} dx \,, \tag{8.3}$$

JHEP07(2002)052

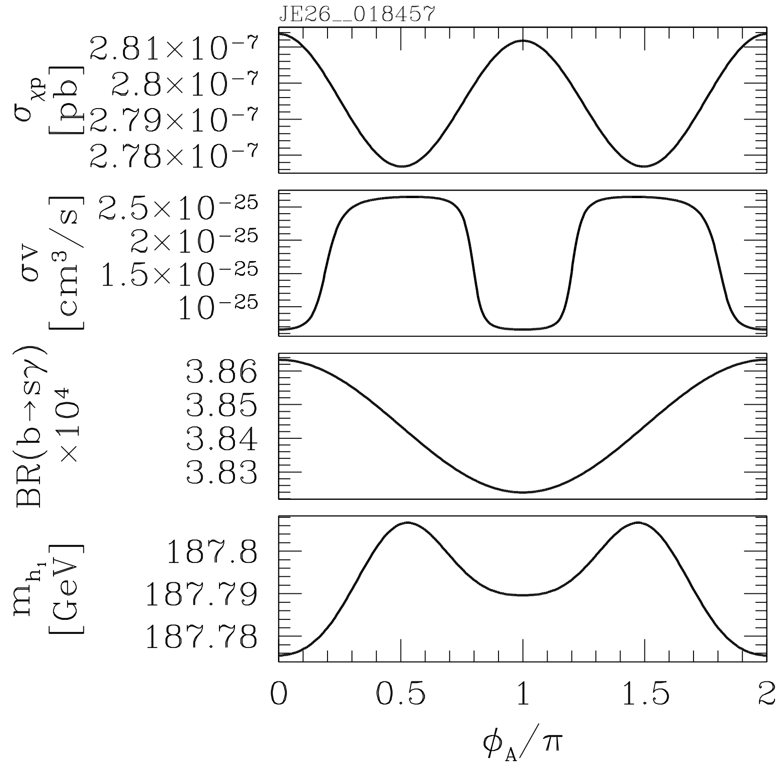

Figure 11: Same notation as figure 8. This case is experimentally allowed for all values of the phase ϕ_A. The annihilation cross section is enhanced by a factor of 4.5 due to CP violation, as can be seen in the second panel. The scattering cross section is in the range accessible to future dark matter experiments.

where $\langle \sigma v \rangle$ is the thermally averaged cross section. For the simple case of s-wave annihilation with constant cross section independent of velocity, J can be replaced by a constant. Hence, far from resonance, we may take

$$\Omega_{NR} h^2 = \frac{1.02 \times 10^{-27}\,\mathrm{cm}^3/\mathrm{s}}{g_*^{1/2} (\sigma v)_{NR} T_f/m}\,, \tag{8.4}$$

where $(\sigma v)_{NR}$ is the constant cross section far from resonance. However, when there is a resonance, the integral J must be calculated more carefully, as previously discussed by [47] and [48]. We follow a similar analysis here.

If $(\sigma v)_{\rm pole}$ is the cross section exactly at the pole, then the Breit-Wigner form for the cross section near a resonance of mass m_R and width Γ_R is

$$\sigma v = (\sigma v)_{NR} + (\sigma v)_{\rm pole} \frac{\Gamma_R^2 m_R^2}{(s - m_R^2)^2 + \Gamma_R^2 m_R^2}\,, \tag{8.5}$$

where $s = 4m_\chi^2/(1 - v^2/4)$ is the Mandelstam variable and v is the relative velocity in the center-of-mass frame (taken to be 0 today). For use in relic abundance calculations, the cross section must be thermal averaged. Once this is done, J can be written as

$$J = \int_0^\infty dv v (\sigma v)\, \mathrm{erfc}\left(v \frac{\sqrt{x_f}}{2} \right). \tag{8.6}$$

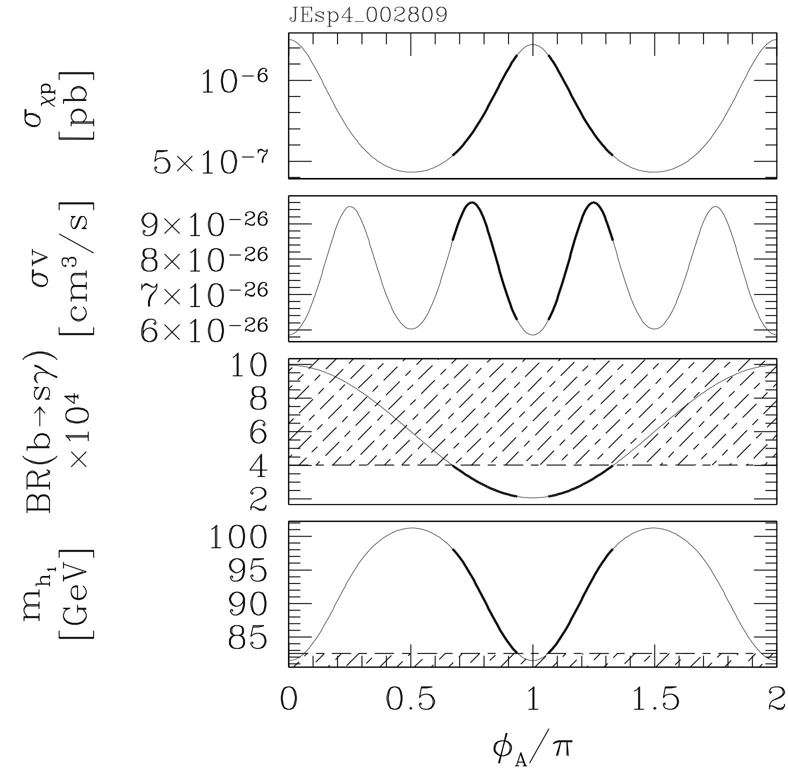

Figure 12: Same notation as figure 8. Here, both CP conserving cases are experimentally excluded while some CP-violating cases are allowed. This is one of the red (dark) points in figure 5. The scattering cross section is of the order of 10^{-6} pb, and lies in the region being probed by direct detection experiments. The annihilation cross section peaks at $\phi_A = 3\pi/4$; notice that this value is not the point of maximal CP violation $\phi_A = \pi/2$.

Here (σv) is the unaveraged cross section and erfc is the complementary error function.

Now using eqs. (8.1), (8.6), (8.4), and (8.5), we may write

$$\frac{(\sigma v)_R}{(\sigma v)_{NR}} = \left(\frac{\Omega_{NR}}{\Omega_\chi} - 1\right) K \tag{8.7}$$

with

$$K = \left[x_f \int_0^\infty dv v \,\mathrm{erfc}\left(v\frac{\sqrt{x_f}}{2}\right) \frac{\epsilon + (u-1)^2}{\epsilon + [u/(1-v^2/4) - 1]^2}\right]^{-1}, \tag{8.8}$$

where we have defined scaled variables

$$u = \left[\frac{2m_\chi}{m_R}\right]^2 \qquad \text{and} \qquad \epsilon = \left[\frac{\Gamma_R}{m_R}\right]^2. \tag{8.9}$$

Now for a resonance of a certain width Γ_R and a given decrease in relic density from the non-resonant value, Ω_χ/Ω_{NR}, we may calculate the maximum enhancement of the cross section over its non-resonant value, $(\sigma v)_R/(\sigma v)_{NR}$, as a function of the number of widths away from the pole,

$$n = \frac{2m - m_R}{\Gamma_R}\,. \tag{8.10}$$

JHEP07(2002)052

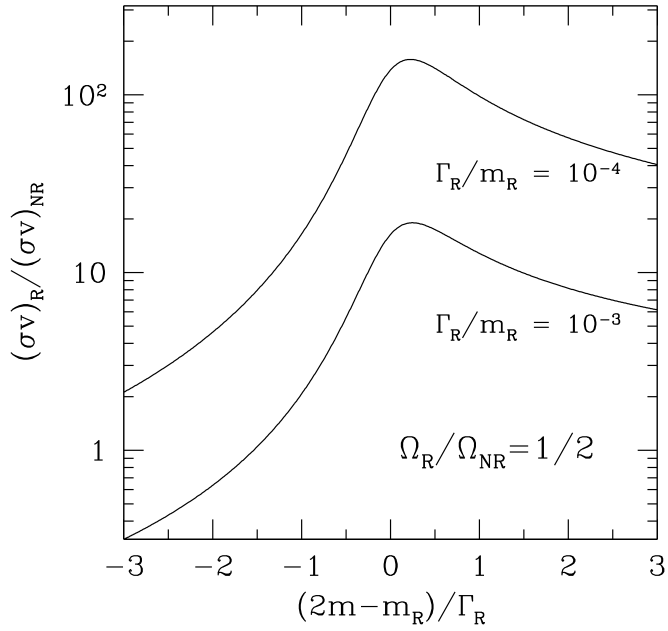

Figure 13: Resonant enhancement of the cross section for neutralino annihilation as a function of the neutralino mass m in units of the resonance width Γ_R. Here m_R is the resonance mass. The two curves are for $\Gamma_R/m_R = 10^{-3}$ and $\Gamma_R/m_R = 10^{-4}$ (the former applies to the model in figure 9).

In figure 13 we have plotted this enhancement for $\Omega_\chi/\Omega_{NR} = 1/2$ (i.e. we have plotted K) for the two values of $\Gamma_R/m_R = 10^{-3}$ and 10^{-4}. From eq. (8.7) we can see that the maximum enhancement for all other values of Ω_χ/Ω_{NR} can then be obtained from the figure by simple scaling, since $(\sigma v)_R/(\sigma v)_{NR} \propto (\frac{\Omega_{NR}}{\Omega_\chi} - 1)$. From this plot, we can see the first category of cases mentioned above. Here we have the relic density changing very little (only a factor of 2) while the annihilation cross section can be enhanced by factors of 10–100. Indeed the new resonances due to CP violation can produce enhancements of 10–100 without much affecting the relic density.

Next we turn to the second category mentioned above. In these cases, the enhancement in σv is large, and the resulting relic density is inversely proportional to the annihilation cross section, $(\sigma v)_R/(\sigma v)_{NR} \simeq K(\Omega_{NR}/\Omega_\chi)$, as can be seen from eq. (8.7) when the 1 in the first term can be neglected. The constant of proportionality K (plotted in figure 13) depends on the resonance width and on the number of widths away from the pole. On resonance, i.e. $2m_\chi = m_R$, K is at least 10 for the narrow Higgs boson resonances that appear in our study. The model in figure 9 is an example of this case. In this model, the Higgs mass is $m_R \simeq 110\,\mathrm{GeV}$ and the Higgs width is $\Gamma_R \simeq 10$ MeV, corresponding to $\epsilon = 10^{-6}$. Here we can run DarkSUSY to conclude that $\Omega_{NR} \sim 10^4$, so that the CP conserving version of these parameters is cosmologically impossible. However, due to the resonant induced amplification of the cross section by a factor of 10^6, the cosmic abundance is brought down to an acceptable value of $\Omega_\chi \sim 0.1$.

In conclusion, there are two interesting regimes of parameter space which do have enhanced annihilation cross sections and also have cosmologically interesting abundances

JHEP07(2002)052

in the range $0.025 < \Omega_\chi < 1$: (1) enhancements of σv by factors of 10 to 100 with only small decreases in Ω_χ, and (2) enhancements of σv by larger factors with decreases in Ω smaller by an order of magnitude.

Partial studies of the neutralino relic density in the presence of CP-violating phases have been done in the context of supergravity [50] or string-inspired models [51], but a full numerical study appropriate to the parameters of this paper is still lacking.

8.4.2 Direct detection

Regarding direct detection searches, those that employ spinless nuclei are directly affected by the suppressions we find in the spin-independent neutralino–proton cross section. This is the case of enriched detectors like ^{73}Ge [49], which have almost exclusively spinless nuclei. The suppression factor for such detectors would be equal to the suppression in the scattering cross section. This is the case with the strongest effect. For all experiments in the foreseeable future, as seen in figure 3, the cross section is reduced by at most a factor of 3, and may be enhanced by a factor of up to 2. In future experiments capable of probing cross sections lower than 10^{-10} pb, the suppression off spinless nuclei can be enormous, up to factors of 10^{-7}.

On the other hand, detectors which contain a fraction of nuclei with spin would still be sensitive to the spin-dependent part of the scattering cross section, which in general is not suppressed simultaneously to the spin-independent cross section. Anyhow, because the spin-independent cross section with nuclei is proportional to the square of the number of nucleons A while the spin-dependent cross section is not, the experimental sensitivity is greatly reduced, by factors of more than $1/A^2 \approx 1000$, when the spin-independent part is suppressed. Hence, in the case when spin-dependent interaction dominates, the suppression in the detection rate is limited to factors of 1000.

8.4.3 Indirect detection

Indirect detection searches are of two types: those looking for neutrinos from neutralino annihilation in the Sun [2] or the Earth [3], and those looking for anomalous cosmic rays or neutrinos from annihilation in the galactic halo [4] or the galactic center [5]. The latter signals are directly proportional to the neutralino annihilation cross section at $v = 0$, and so are proportionally affected by the enhancements and suppressions we find when we allow for CP-violating phases in A. In other words, indirect detection rates from the galactic halo or center can be increased by factors of typically one to four and occasionally of up to 10^6.

Indirect detection from the Earth or the Sun is more complicated. As we will argue, a non-zero value of $\mathrm{Im}(A)$ can change the indirect detection rate in either direction. Decreased scattering cross sections lead to decreased indirect signals from the Earth or the Sun, while increased annihilation cross sections lead to increased indirect signals from the Earth or the Sun. We recall the idea behind indirect detection. Neutralinos residing in the galactic halo pass through the Sun or Earth and some of them get captured. Then they sink to the center of the Sun or Earth, where they annihilate with one another to give neutrino signals detectable in neutrino detectors on the surface of the Earth. It is clear that in this process, both scattering and annihilation cross sections are of crucial importance. The maximal observable neutrino signal occurs when equilibrium is reached between capture of particles and their annihilation. In this case the final neutrino signal depends only on the capture rate, and so on the scattering cross section of neutralinos with the nuclei in the Sun or the Earth. In the Sun, the most important nuclei for neutralino capture are oxygen and hydrogen. Oxygen has zero spin; hydrogen has spin-1/2. When the spin-independent scattering cross section is suppressed, neutralinos can still be captured in the Sun by scattering off of hydrogen. Therefore we expect only a small suppression in the capture rate in the Sun, and hence in the neutrino signals from the Sun in the case where equilibrium is reached. On the other hand, capture by the Earth is essentially due to scattering off of spinless nuclei, such as iron and nickel. Big suppressions in the spin-independent cross section are therefore expected to lead to big suppressions in the capture rate in the Earth, and hence in the neutrino signals from the Earth in the case where equilibrium is reached.

However, equilibrium may not have been reached in the age of the solar system between capture of neutralinos and their annihilation in the Earth or Sun. The timescale for equilibration is $\tau = (CC_A)^{-1/2}$, where C is the capture rate and C_A is the annihilation rate. Here, C is proportional to the neutralino–nucleon scattering cross section and C_A is proportional to the neutralino annihilation cross section. Again, a suppressed scattering cross section goes in the direction of suppressing the indirect detection rate: the capture rate is smaller, the timescale for equilibration is longer, and the neutrino flux is not at full strength. However, a non-zero value of $\mathrm{Im}(A)$ may also lead to an enhanced annihilation cross section; this enhancement goes in the opposite direction of driving the system towards equilbrium more quickly. When the annihilation rate is bigger, the timescale for equilibration is smaller, and the system is driven towards full signal more quickly. Hence an enhanced annihilation rate should increase the indirect detection rate from the Earth in those cases where annihilation was not ordinarily reached (for $\mathrm{Im}(A) = 0$).

In conclusion, we expect that decreased scattering cross sections lead to decreased signals for direct detection and indirect detection from the Sun or the Earth, while increased annihilation cross sections lead to increased signals for indirect detection.

A detailed study of the consequences of the present results on the neutralino relic density and on direct and indirect searches of neutralino dark matter is an interesting topic for future study.

9. Conclusions

We have examined the effect of CP violation on the neutralino annihilation and scattering cross sections, which are of importance in calculations of the neutralino relic density and of the predicted rates for direct and indirect searches of neutralino dark matter. Specifically we have considered the case in which the only CP-violating phase in addition to the standard model CKM phase is in the complex soft trilinear scalar couplings A of the third generation. This phase affects the squark masses and through radiative corrections generates a mixing between CP-even and CP-odd Higgs bosons. This mixing modifies the neutralino annihilation and scattering cross sections in the kinematic regimes relevant for dark matter detection. Exploring $\sim 10^6$ points in supersymmetric parameter space with a non-zero phase of A, we have found that: (1) the scattering cross section may be enhanced by a factor of up to 2; (2) the scattering cross section is generally suppressed, up to factors of 3 in the range accessible to detectors in the foreseeable future, and even by 7 orders of magnitude for lower cross sections; (3) the annihilation cross section can be enhanced. Typical enhancements are a factor of one to four, but may be as large as 10^6 in the case of resonant annihilation when the neutralino mass is close to half the Higgs mass. Two possibilities exist when the mass is on resonance: (i) in some cases enhancement by factors of up to 100 is possible without much changing the value of the relic density, while (ii) in other cases the relic density is brought down by many orders of magnitude to a cosmologically viable range and the annihilation cross section is brought up to an experimentally accessible value. We have also found cases which are experimentally or cosmologically excluded when CP conservation is imposed but are allowed when CP conservation is violated. Some of these cases have neutralino masses and cross sections in the region probed by current dark matter searches. Decreased scattering cross sections may lead to decreased signals for direct detection and indirect detection from the Sun or the Earth, while increased annihilation cross sections may lead to increased signals for indirect detection.

Acknowledgments

We would like to thank the Department of Energy for support through the Physics Department at the University of Michigan, and the Max Planck Institut für Physik for support during the course of this work. We thank Apostolos Pilaftsis, Tobias Hurth, and Pietro Antonio Grassi for helpful discussions.

References

[1] M.W. Goodman and E. Witten, *Detectability of certain dark-matter candidates*, *Phys. Rev.* **D 31** (1985) 3059.

[2] J. Silk, K.A. Olive and M. Srednicki, *The photino, the sun and high-energy neutrinos*, *Phys. Rev. Lett.* **55** (1985) 257.

[3] K. Freese, *Can scalar neutrinos or massive dirac neutrinos be the missing mass?*, *Phys. Lett.* **B 167** (1986) 295;
L.M. Krauss, M. Srednicki and F. Wilczek, *Solar system constraints and signatures for dark matter candidates*, *Phys. Rev.* **D 33** (1986) 2079.

[4] J.E. Gunn, B.W. Lee, I. Lerche, D.N. Schramm and G. Steigman, *Some astrophysical consequences of the existence of a heavy stable neutral lepton*, *Astrophys. J.* **223** (1978) 1015;
F.W. Stecker, *The cosmic gamma ray background from the annihilation of primordial stable neutral heavy leptons*, *Astrophys. J.* **223** (1978) 1032.

[5] P. Gondolo and J. Silk, *Dark matter annihilation at the galactic center*, *Phys. Rev. Lett.* **83** (1999) 1719 [astro-ph/9906391].

[6] T. Falk, A. Ferstl and K.A. Olive, *New contributions to neutralino elastic cross-sections from CP-violating phases in the MSSM*, *Phys. Rev.* **D 59** (1999) 055009 [hep-ph/9806413].

[7] S. Dimopoulos and G.F. Giudice, *Naturalness constraints in supersymmetric theories with nonuniversal soft terms*, *Phys. Lett.* **B 357** (1995) 573 [hep-ph/9507282];
A. Cohen, D.B. Kaplan and A.E. Nelson, *The more minimal supersymmetric standard model*, *Phys. Lett.* **B 388** (1996) 588 [hep-ph/9607394];
A. Pomarol and D. Tommasini, *Horizontal symmetries for the supersymmetric flavor problem*, *Nucl. Phys.* **B 488** (1996) 3 [hep-ph/9507462];
S. Khalil, T. Kobayashi and O. Vives, *Edm-free supersymmetric CP-violation with non-universal soft terms*, *Nucl. Phys.* **B 580** (2000) 275 [hep-ph/0003086];
S.A. Abel and J.M. Frère, *Could the MSSM have no CP violation in the CKM matrix?*, *Phys. Rev.* **D 55** (1997) 1625 [hep-ph/9608251];
U. Chattopadhyay, T. Ibrahim and D.P. Roy, *Electron and neutron electric dipole moments in the focus point scenario of sugra model*, *Phys. Rev.* **D 64** (2001) 013004 [hep-ph/0012337].

[8] A. Pilaftsis, *Higgs scalar-pseudoscalar mixing in the minimal supersymmetric standard model*, *Phys. Lett.* **B 435** (1998) 88 [hep-ph/9805373].

[9] H.E. Haber, in Particle Data Group, *Review of particle properties*, *Eur. Phys. J.* **C 3** (1998) 1.

[10] S. Dimopoulos and S. Thomas, *Dynamical relaxation of the supersymmetric CP-violating phases*, *Nucl. Phys.* **B 465** (1996) 23 [hep-ph/9510220].

[11] L. Bergström and P. Gondolo, *A lead astronomical neutrino detector: land*, *Astropart. Phys.* **5** (1996) 183.

[12] A. Bottino and N. Fornengo, *Dark matter and its particle candidates*, hep-ph/9904469.

[13] G. Jungman, M. Kamionkowski, and K. Griest, *Supersymmetric dark matter*, *Phys. Rept.* **267** (1996) 195 [hep-ph/9506380].

[14] J. Edsjö and P. Gondolo, *Neutralino relic density including coannihilations*, *Phys. Rev.* **D 56** (1997) 1879 [hep-ph/9704361].

[15] L. Bergström, P. Ullio and J. H. Buckley, *Observability of gamma rays from dark matter neutralino annihilations in the milky way halo*, *Astropart. Phys.* **9** (1998) 137 [astro-ph/9712318].

[16] P. Gondolo, J. Edsjö, L. Bergström, P. Ullio and E.A. Baltz, *DarkSUSY - A numerical package for dark matter calculations in the MSSM,* talk presented at Identification of Dark Matter (IDM2000), York, England, September 1999.

[17] J.R. Ellis, G. Ridolfi and F. Zwirner, *On radiative corrections to supersymmetric Higgs boson masses and their implications for LEP searches*, *Phys. Lett.* **B 262** (1991) 477.

[18] A. Blondel, F. Gianotti, Y. Gao and P. Gay, ALEPH collaboration, in *High Energy Physics 99*, Tampere, Finland, July 1999 http://alephwww.cern.ch/ALPUB/conf/conf.html.

[19] S. Bertolini, F. Borzumati, A. Masiero and G. Ridolfi, *Effects of supergravity induced electroweak breaking on rare B decays and mixings*, *Nucl. Phys.* **B 353** (1991) 591.

[20] D. Chang, W.-Y. Keung and A. Pilaftsis, *New two-loop contribution to electric dipole moment in supersymmetric theories*, *Phys. Rev. Lett.* **82** (1999) 900 [hep-ph/9811202].

[21] A. Manohar and H. Georgi, *Chiral quarks and the nonrelativistic quark model*, *Nucl. Phys.* **B 234** (1984) 189.

[22] T. Ibrahim and P. Nath, *The neutron and the electron electric dipole moment in $N = 1$ supergravity unification*, *Phys. Rev.* **D 57** (1998) 478 [hep-ph/9708456].

[23] E.D. Commins, S.B. Ross, D. DeMille and B.C. Regan, *Improved experimental limit on the electric dipole moment of the electron*, *Phys. Rev.* **A 50** (1994) 2960.

[24] I.S. Altarev et al., *Search for the neutron electric dipole moment*, *Phys. Atom. Nucl.* **59** (1996) 1152.

[25] Particle Data Group, C. Caso et al., *Review of particle physics*, *Eur. Phys. J.* **C 3** (1998) 1; 1999 partial update for edition 2000 (http://pdg.lbl.gov).

[26] OPAL collaboration, G. Abbiendi et al., *Search for Higgs bosons in e^+e^- collisions at 183 GeV*, *Eur. Phys. J.* **C 7** (1999) 407.

[27] ALEPH collaboration, J. Carr et al., *ALEPH status report*, talk to LEPC, 31 March 1998 http://alephwww.cern.ch/ALPUB/seminar/carrlepc98/index.html.

[28] L3 collaboration, M. Acciarri et al., *Search for supersymmetric particles at $130\,GeV < \sqrt{s} < 140\,GeV$ at LEP*, *Phys. Lett.* **B 377** (1996) 289.

[29] ALEPH collaboration, D. Decamp et al., *Searches for new particles in Z decays using the ALEPH detector*, *Phys. Rept.* **216** (1992) 253.

[30] K. Hidaka, *Absolute mass limits of gaugino-higgsino sector in minimal supersymmetric model from LEP and CDF data*, *Phys. Rev.* **D 44** (1991) 927.

[31] L3 collaboration, M. Acciarri et al., *Search for neutralinos in Z decays*, *Phys. Lett.* **B 350** (1995) 109.

[32] ALEPH collaboration, D. Buskulic et al., *Mass limit for the lightest neutralino*, *Z. Physik* **C 72** (1996) 549 [hep-ex/9607009].

[33] L3 collaboration, M. Acciarri et al., *Search for scalar leptons, charginos and neutralinos in e^+e^- collisions at $\sqrt{s} = 161$ GeV to 172 GeV*, *Eur. Phys. J.* **C 4** (1998) 207.

[34] OPAL collaboration, G. Abbiendi et al., *Search for chargino and neutralino production at $\sqrt{s} = 181$ GeV–184 GeV at LEP*, *Eur. Phys. J.* **C 8** (1999) 255.

[35] D0 collaboration, S. Abachi et al., *Search for squarks and gluinos in $p\bar{p}$ collisions at $\sqrt{s} = 1.8$ TeV*, *Phys. Rev. Lett.* **75** (1995) 618.

[36] CDF collaboration, F. Abe et al., *Search for gluinos and squarks at the Fermilab Tevatron collider*, *Phys. Rev.* **D 56** (1997) R1357.

[37] CDF collaboration, F. Abe et al., *Search for squarks and gluinos from $\bar{p}p$ collisions at $\sqrt{s} = 1.8$ TeV*, *Phys. Rev. Lett.* **69** (1992) 3439.

[38] CDF collaboration, F. Abe et al., *Search for gluino and squark cascade decays at the Fermilab Tevatron collider*, *Phys. Rev. Lett.* **76** (1996) 2006.

[39] ALEPH collaboration, R. Barate et al., *Search for sleptons in e^+e^- collisions at centre-of-mass energies up to 184 GeV*, *Phys. Lett.* **B 433** (1998) 176.

[40] J. Gasser, H. Leutwyler and M.E. Sainio, *Sigma term update*, *Phys. Lett.* **B 253** (1991) 252; M. Drees and M. Nojiri, *Phys. Rev.* **D 48** (1993) 3483.

[41] R. Bernabei et al., *New limits on wimp search with large-mass low-radioactivity NAI(TL) set-up at gran sasso*, *Phys. Lett.* **B 389** (1996) 757.

JHEP07(2002)052

[42] CDMS collaboration, R. Abusaidi et al., *Exclusion limits on the wimp nucleon cross-section from the cryogenic dark matter search*, *Nucl. Instrum. Meth.* **A444** (2000) 345 [astro-ph/0002471].

[43] CDMS collaboration, R. Schnee, talk presented at *Inner space/outer space II*, Fermilab, May 1999.

[44] CRESST-COLLABORATION collaboration, M. Bravin et al., *The cresst dark matter search*, *Astropart. Phys.* **12** (1999) 107 [hep-ex/9904005].

[45] L. Baudis et al., *Genius: a new dark matter project*, *Phys. Rept.* **307** (1998) 301.

[46] V. Mandic, A. Pierce, P. Gondolo, and H. Murayama, in preparation.

[47] K. Griest and D. Seckel, *Three exceptions in the calculation of relic abundances*, *Phys. Rev.* **D 43** (1991) 3191.

[48] P. Gondolo and G. Gelmini, *Cosmic abundances of stable particles: improved analysis*, *Nucl. Phys.* **B 360** (1991) 145.

[49] F. Avignone, private communication.

[50] T. Falk, K.A. Olive and M. Srednicki, *Phases in the MSSM, electric dipole moments and cosmological dark matter*, *Phys. Lett.* **B 354** (1995) 99 [hep-ph/9502401];
T. Falk and K.A. Olive, *More on electric dipole moment constraints on phases in the constrained MSSM*, *Phys. Lett.* **B 439** (1998) 71 [hep-ph/9806236].

[51] S. Khalil and Q. Shafi, *Supersymmetric phases and the LSP relic density and detection rates*, *Nucl. Phys.* **B 564** (1999) 19 [hep-ph/9904448].